Summer 2009

Numerical/Experimental Investigation of Plunge Stage and Effect of Donor Material in Friction Stir Welding

Saptarshi Mandal
Old Dominion University

NUMERICAL/EXPERIMENTAL INVESTIGATION OF PLUNGE STAGE AND EFFECT OF DONOR MATERIAL IN FRICTION STIR WELDING

by

Saptarshi Mandal
B.E. August 2000, Marine Engineering & Research Institute, India
M.S. August 2003, Old Dominion University

A Dissertation Submitted to the Faculty of
Old Dominion University in Partial Fulfillment of the
Requirement for the Degree of

DOCTOR OF PHILOSOPHY

MECHANICAL ENGINEERING

OLD DOMINION UNIVERSITY
August 2009

Approved by:

Abdelmageed A. Elmustafa (Director)

Gene J. Hou (Member)

Stephen C. Cupschalk (Member)

Keith M. Williamson (Member)

Numerical/Experimental Investigation of the Plunge Stage and Effect of Donor Material in Friction Stir Welding

Saptarshi Mandal
Old Dominion University, 2009
Director of Advisory Committee: Dr. A.A. Elmustafa

Friction Stir Welding (FSW) was developed in 1991 as a robust solid-state joining technique that uses a specially shaped rotating tool to generate heat and plasticize material around the tool. The tool then mixes plasticized material along the joint line to produce the weld. Over the last decade, FSW has become increasingly popular for welding aluminum. The combination of attractive properties of the weld and cost-efficiency has led researchers to investigate the feasibility of using FSW for steel. One of the major impediments for using friction stir welding for harder materials such as steel is tool wear. It is well-documented that a large part of this wear occurs during the initial plunge phase. This dissertation focuses on developing a better understanding of the plunge stage of FSW and also proposes a novel concept to mitigate tool wear during plunge. The commercial FEA code, ABAQUS is used to simulate the plunge phase and the results are compared with experimental results obtained from literature. Plunge experiments on AA 2024 were also conducted during the course of this research and the axial load and temperature were measured. The 'donor material' concept was proposed for the reduction of tool wear at the plunge by providing localized pre-heating at the plunge area using a softer material as a 'donor.' This process creates heat in a relatively soft 'donor' material, which is transferred to the much harder workpiece material by conduction. The expected advantage of this localized process is that it reduces the chances of altering the microstructure of the base material due to excessive heat, which is

a possibility in conventional pre-heating methods. This research includes several numerical simulations of the donor material concept with different donor materials and plain carbon steel as the workpiece. It was observed in the case of using a donor material that the axial load during the plunge decreased by approximately 80%. Additionally, the contact stresses at the tool workpiece interface also decreased by approximately 75% when a donor material was used in the plunge area. Decrease in both the axial force and contact stress should contribute to the decrease of tool wear. Proof of concept experiments are also demonstrated with copper as the donor and AA 2024 as the base material.

This dissertation is dedicated to my parents who have sacrificed a lot in order to help me be the person I am today.

ACKNOWLEDGMENTS

I thank Dr. Elmustafa for his excellent guidance during this dissertation. He has been a source of constant support and encouragement right through the process especially during the hard times. Without his advice this dissertation would not be possible. Dr. Williamson introduced me to the field of friction stir welding and encouraged me to join the doctoral program for which I am extremely grateful to him. I thank Dr. Cupschalk for his constant support during this work and also for sharing his in-depth knowledge of metallurgy. Dr. Hou has helped me a great deal with his thorough knowledge of finite element analysis. Justin Rice has been of tremendous help during this work especially with the experimental areas of research. Also, this research would be impossible without the support of my family and friends who stood by me throughout this journey.

The initial part of this work was supported by the National Science Foundation's Division of Design, Manufacturing & Industrial Innovation under Award #0343646.

TABLE OF CONTENTS

LIST OF TABLES

LIST OF FIGURES

CHAPTER 1

INTRODUCTION

For over a century, fusion welding has been the key joining method used in most industrial applications. Although fusion welding processes such as electric arc welding is efficient for welding ferrous alloys, some difficulties occur during welding aluminum, due to its strong affinity for oxygen. Arc welding aluminum creates oxides and porosity in the weld, which reduces the strength of the joint. Although metal inert gas welding has produced good quality welds in aluminum, recent developments in solid state welding techniques like rotary friction welding and friction stir welding have resulted in high quality and economical welds.

In 1991, The Welding Institute in the United Kingdom developed Friction Stir Welding as a new welding technology, to provide a robust solid-state joining technique for welding aluminum and other alloys [1,2]*. During FSW, a rotating, hardened, non-consumable tool is used to generate frictional heat while simultaneously inducing plastic deformation. The significant differences in material properties between the tool and the workpiece, together with tool's continuous cyclical movement, generate frictional heat resulting in the formation of plasticized conditions ('third body') in the workpiece [3]. FSW has become increasingly popular for joining materials like aluminum, which are difficult to weld by conventional joining techniques. The process is also convenient for joining dissimilar metals. Due to the absence of any kind of melting during FSW,

* References as presented in Journal of Engineering Materials and Technology

oxidation is minimized, thus producing welds with low porosity. Typically, Friction Stir Welding (FSW) produces welds with high joint strength that are at least as good as fusion welds if not better. This can be attributed to the small Heat Affected Zone (HAZ) as compared to the conventional arc welding techniques. This process is easy to automate and once the welding parameters are set, it is highly reproducible, making it an attractive joining solution in industries requiring mass production. Since it is a solid-state process and there is no melt pool that shrinks significantly on solidification, the welds have minimal distortion and very low residual stresses [4]. This also eliminates cracking in the welds. Additionally, FSW does not require filler wire typically required for conventional fusion welding techniques. These advantages combine to make it an attractive process for various applications in the aerospace industry such as fuselages, wings and cryogenic fuel tanks for space shuttles. In aircrafts, FSW helps to reduce the use of rivets which also reduces the overall weight of the aircraft. Similarly, FSW has applications in high-speed trains, ferry boats and shipbuilding industries.

1.1 *Description of FSW process*

In a typical FSW butt weld, the specially shaped rotating tool is plunged between the abutting faces of the joint to generate localized heat, and create a plasticized area around the immersed region of the tool. Thermomechanical energy within the plasticized region produces the weld. The tool's pin, which is smaller in diameter than the shoulder, traverses along the joint line while the shoulder is in close contact with the workpiece's surface to avoid expelling softened material [1,2]. As the tool moves along the joint, the material is heated and plasticized by the leading edge of the tool and is pushed to the

trailing edge where it hardens to form the FSW joint [2]. The material flow during weld formation can be fairly complex due to the tool's geometric features. Thus, the tool has essentially three functions: a) to generate heat by friction, b) to contain the material in the plasticized area and c) to move the material to form a joint. During the process the material undergoes severe plastic deformation at high temperatures resulting in the generation of fine, equiaxed recrystallized grains [5-8]. The weld formed is fine grained with nominal oxidation and porosity. The process is illustrated in Fig. 1-1.

In the last decade, FSW has emerged as one of the most significant developments in metal joining. It is environmentally friendly, energy efficient and very versatile. As compared to the conventional welding methods, FSW consumes considerably less energy. FSW only consumes 2.5% of the energy of laser welding [9]. No cover gas or flux is used, thereby making the process environmentally friendly. The joining does not involve any use of filler metal and therefore any aluminum alloy can be joined without concern for the compatibility of composition, which is an issue in fusion welding [9]. Also, since FSW does not require any kind of surface cleaning, it eliminates the need for harmful solvents for degreasing and also eliminates grinding wastes. FSW can be applied to a wide variety of joints such as butt joints, lap joints, T joints and fillet welds. The versatility of the process also allows for joining materials of different thickness. Recently, spot welding of thin sheets has become a popular application in the automotive industry. This has the potential to replace a lot of fasteners, leading to a drastic reduction in overall weight, which of course translates to energy efficiency. FSW is also effective in making welds in dissimilar materials [10-12]. Watanabe et al [10] and Uzun et al [11]

successfully joined aluminum alloys with steel using FSW. The tensile strength of the joints was about 86% of the base material [10]. Mishra et al [13-14] recently developed a material processing technique called friction stir processing, which utilizes the advantages of microstructural modification in a friction stir weld. A rotating tool is inserted into a monolithic workpiece and the tool is traversed forward, producing a localized fine microstructure leading to good mechanical properties [13-14].

The success of using FSW to join softer materials has led researchers to investigate the feasibility of using FSW to weld harder materials like steel. Applications for FSW of steel could be beneficial in a variety of industries such as shipbuilding, pipe-fabrication and railways. The U.S. Navy has identified several possible advantages of substituting the conventional fusion welding process with FSW for steels used in naval ship constructions. As mentioned earlier, traditional fusion welding processes can cause severe plate distortion. This is because of large thermal gradients and the formation of a melt pool. FSW being a solid state process eliminates the melt pool and also produces lower peak temperatures resulting in low distortion welds. In general, controlling weld distortions is an expensive process. The U.S. Navy has estimated that the potential cost saving for using FSW, which thereby eliminates the need to control weld distortion, can be as much as $3.4M for DDG-51 class vessel [15,16]. Another significant advantage of FSW is that it does not create the fume associated with arc welding processes. Studies by the U.S. Navy have shown that the fumes created in current shipyard welding practices exceed the proposed Occupational Health and Safety Administration's allowable limit for hexavalent chromium (Cr6+), a known carcinogen [15]. The Navy estimated that keeping

the Cr6+ under the allowable limits would incur a one-time implementation cost of $30M and an annual cost of $80M [15,16]. Using friction stir welding whenever possible would eliminate much of the potential fume and cut the costs of controlling Cr6+ generation. With several obvious advantages, FSW of steel is an attractive option in several industries despite the presence of well-proven fusion welding techniques. Several researchers [3,15,17-19] have already demonstrated the feasibility of joining ferrous materials using FSW. These welds also meet the stringent physical property requirements for ship construction set forth by the Navy [16].

However, tool wear is a significant impediment in obtaining continuous friction stir welds in steel. Although this is not a problem for welding softer materials, it becomes a significant hindrance in producing long, continuous welds in harder materials like steel. This requirement for long continuous welds is an essential parameter for using FSW for manufacturing large units that are typical of shipbuilding and railway industries. The demand for joining harder materials with FSW justifies research on advancing stir-welding techniques for harder materials like steel. Most researchers have focused on two approaches for development. One approach focuses on increasing the tool's hardness while the second approach introduces a pre-heating source ahead of the stir tool. Increasing the tool's hardness could be accomplished by using different coatings such as Tungsten carbides and Polycrystalline Boron Nitride (PCBN). According to Thomas [3], the key to FSW of harder materials such as steel is maintaining a suitable differential in the hardness of both the work-piece material and the stir tool at elevated temperatures. However, this could significantly increase the price of fabricating tools that are already

expensive. Also, the interaction of the tool material with the workpiece at high temperatures is rather complex and is not yet fully understood. An alternative approach is to pre-heat the workpiece prior to stir welding [4-7]. This approach is based on the idea that pre-heating the workpiece reduces the flow stresses and softens the material and thus reduces wear when the tool is plunged into it. It has also been documented that a significant fraction of the tool wear occurs during the initial plunge phase of the weld [3, 19-21].

The plunge stage in friction stir welding (FSW) process is extremely critical since most of the initial thermomechanical conditions are generated and the material undergoes significant transformation due to the high temperatures and stresses involved in the process. The highly dynamic nature of this phase makes it a challenging research area. A thorough understanding of the plunge stage is also important in the development of tools and processes for successfully stir welding high strength alloys like steel and titanium-based alloys, as most of the tool wear occurs during this phase [3, 19-21]. This warrants the need for more experimental and numerical research to investigate material processes during this stage.

This dissertation focuses on developing a better understanding of the plunge stage of FSW both numerically and experimentally. The literature review provides an in-depth insight on the various numerical modeling performed by various researchers and also highlights why the numerical model presented in this research is unique. The review also presents various experimental and numerical FSW studies on steel and also reviews tool

wear in case of FSW. The next chapters focus on the development of a numerical model for the plunge phase in FSW and also present experiments conducted during the current research and its comparison to the numerical model. Based on this research of the plunge stage, a novel concept is proposed to provide localized pre-heating at the plunge area using a softer material as a 'donor.' This process creates heat in a relatively soft 'donor' material, which is transferred to the much harder workpiece material by conduction. The expected advantage of this localized process is that it reduces the chances of altering the micro-structure of the base material by supplying excessive heat, which could negate the advantage of FSW in producing good joints with properties similar to the base material. This research includes several numerical simulations of the donor material concept with different donor materials and plain carbon steel as the workpiece. A proof of concept experiment is also demonstrated.

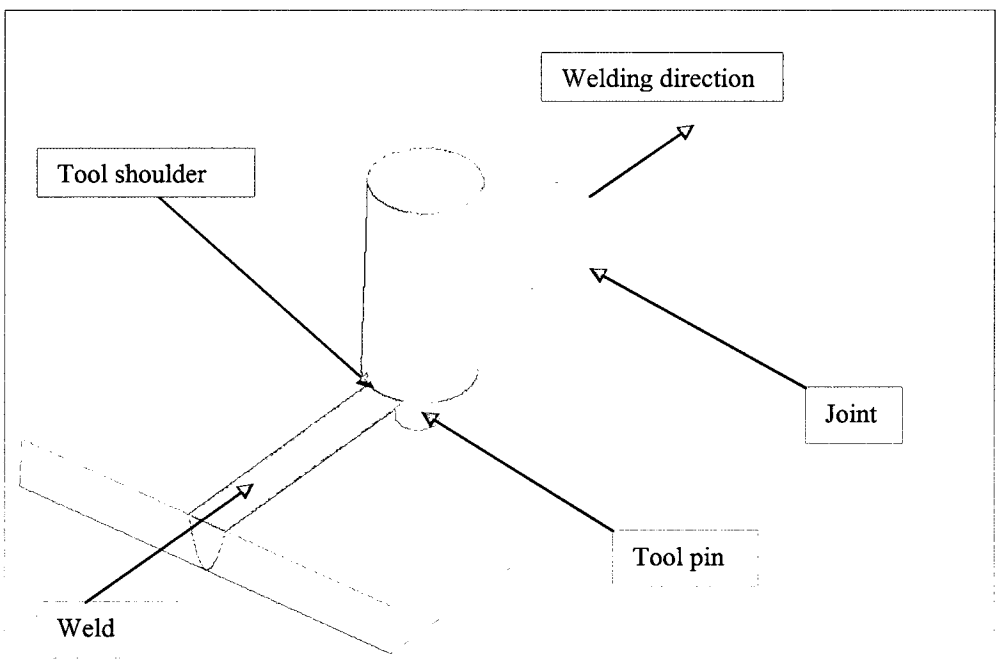

Fig.1-1. Schematic of a FSW process

References

1. Thomas, W., Nicholas, E.D., Needham, J.C., Murch, M.G., Templesmith, P., Dawes, C.J., G.B. Patent Application No. 9125978.8 (December 1991).

2. Dawes, C.J., Thomas, W., *TWI Bulletin 6*, November/December 1995, p. 124.

3. Thomas, W., "Friction Stir Welding of Ferrous Materials; A Feasibility Study" *Proceedings of First International Symposium on Friction Stir Welding,* Thousand Oaks, California, 14-16 June 1999.

4. Johnson, R. and Kallee, S., 1999, "Friction Stir Welding" *Materials World*, Vol. 7, pp. 751-53.

5. Rhodes, C.G., Mahoney, M.W., Bingel, W.H., Spurling, R.A., Bampton, C.C., 1997, "Effects of friction stir welding on microstructure of 7075 aluminum" *Scripta Materiala*, pp. 69-75.

6. Liu, G., Murr, L.E., Niou, C.S., McClure, J.C., Vega, F.R., 1997, "Microstructural aspects of the friction-stir welding of 6061-T6 aluminum" *Scripta Materialia*, pp. 355-361.

7. Jata, K.V., Semiatin, S.L., 2000, "Continuous dynamic recrystallization during friction stir welding of high strength aluminum alloys" *Scripta Materialia*, pp.743-749.

8. Benavides, S., Li, Y., Murr, L.E., Brown, D., McClure, J.C., 1999, "Low-temperature friction-stir welding of 2024 aluminum" *Scripta Materiala*, pp.809-815.

9. Mishra, R., Ma, Z.Y., 2005, "Friction stir welding and processing", *Materials Science and Engineering R*, pp.1-78.

10. Watanabe, T., Takayama' H., Yanagisawa, A., 2006, "Joining of aluminum alloys to steel by friction stir welding", *Journal of Materials Processing Technology*, pp. 342-349.

11. Uzun, H., Donne, C. D., Argagnotto, A., Ghidini, T., Gambaro, C., 2005, "Friction stir welding of dissimilar Al 6013-T4 To X5CrNi18-10 stainless steel", *Materials & Design*, pp. 41-46.

12. Kwon, Y.J., Shigematsu, I., Saito, N., 2008, "Dissimilar friction stir welding between magnesium and aluminum alloys", *Materials Letters*, pp. 3827-3829.

13. Mishra, R.S., Mahoney, M.W., McFadden, S.X., Mara, N.A., Mukherjee, A.K., 2000, "High strain rate superplasticity in a friction stir processed 7075 Al alloy" *Scripta Materialia*, pp.163-168.

14. Mishra, R.S., Mahoney, M.W., 2001, "Friction stir processing: A new grain refinement technique to achieve high strain rate superplasticity in commercial alloys" *Material Science Forum*, pp.357–359.

15. Posada, M., Nguyen, J.P., Forrest, D.R., DeLoach, J.J. and DeNale, R., "Friction stir welding advances joining technology" *AMPTIAC*, Vol. 7, No. 3, pp. 13-20.

16. Norton, S.J., 2006, "Ferrous FSW physical simulation" *PhD Dissertation*, Ohio State University.

17. Konkol, P.J., Mathers, J.A., Johnson, R., Pickens, J.R., "Friction stir welding of HSLA-65 [high strength low alloy] steel for shipbuilding" *Proceedings of Friction Stir Welding, 3rd International Symposium*, Kobe, Japan, 27-28 September 2001.

18. Nelson, T.W., Su, J.-Q., Steel, R.J., "Friction stir welding of ferritic steels" *The 14th International Offshore and Polar Engineering Conference*, Toulon, France, May 23-28, 2004 .

19. Lienert T.J., Stellwag W.L. Jr., Grimmett, B.B., Warke, R.W., 2003, "Friction stir welding studies on mild steel" *Supplement to the Welding Journal*, pp.1s-9s.

20. Thomas, W., 1999, "Feasibility of Friction Stir Welding Steel" *Science and Technology of welding and joining,* Vol. 4, pp. 365-372.

21. Mandal, S., Williamson, K., 2006, "A thermomechanical hot channel approach for friction stir welding" *Journal of Materials Processing Technology*, pp.190-194.

22. Mandal, S., 2003, "Analytical model of a thermomechanical hot channel coupled to a friction stir welding process" *M.S. Thesis*, Old Dominion University.

Chapter 2

LITERATURE REVIEW

Although Friction Stir Welding has been largely confined to relatively soft materials such as aluminum alloys and lead and zinc, the feasibility of the process has been demonstrated on harder materials such as low carbon and stainless steels [1,2,3]. With the development of a feasible technology for stir welding steels, FSW could be used for important commercial applications like ship building and automobile production. However, the production of continuous long stir welds in harder materials such as steel, and manganese has been significantly hampered by limited tool life due to wear and tear. Frequent replacement of worn out tools is an expensive process and increases the production time due to tool changes. Researchers have also observed that the majority of the wear occurs during the time the tool plunges into the workpiece material [1,2,3]. This makes the plunge phase a very critical area of research. Although, a significant amount of research has primarily focused on the actual welding phase of FSW, very little research, both experimental and numerical has been conducted on the plunge. The primary focus of this research as mentioned earlier is to develop a better understanding of the plunge and its relation to wear. It also proposes a novel localized pre-heating approach to mitigate tool wear during plunge. The study uses both numerical simulations as well as experiments towards this goal.

This research would be incomplete without reviewing the work of other researchers and the significant contributions they have made. This chapter reviews some of the FEA-based simulation models developed for FSW. The highly dynamic nature of this phase makes it a very interesting yet challenging problem. Some of the experiments on high hardness materials are discussed as well as the challenges in performing them. A discussion on tool wear based on experiments performed by researchers is included which is very pertinent to this research. Finally, some of the approaches adopted by various researchers to tackle the problem of tool wear are discussed.

2.1 *Review of numerical simulations*

FSW results in intense plastic deformation and high temperatures not only in the stir zone but also in the regions surrounding it. It is critical that an understanding of the mechanical and thermal processes during FSW be developed for optimizing the process parameters and controlling the welds' microstructures and properties. Numerical modeling is an important tool for predicting and optimizing the FSW process. It is relatively inexpensive and also provides an insight into areas which are usually difficult to quantify in an experimental investigation like temperatures at the contact interface, flow stress, strain rates, etc. However, numerical simulations could be costly depending on the computational time. The most general FSW model would include both an elastic and plastic response, and features full mechanical and thermal coupling. However, due to computational costs, several simplifications are made to reduce the complexity of the FSW problem. The simulations need to be optimized so that they provide the required information and yet converge in a reasonable amount of time. A significant amount of

work has been done in numerical simulations of FSW. Most of these can be broadly classified into either computational fluid dynamics (CFD) [4-7] or solid mechanics [8-14] models. The solid mechanics models in FSW are usually either elastic-viscoplastic, which include both the elastic and plastic response of the material or rigid-viscoplastic which neglect the elastic response of the material. Since the plastic strains produced in FSW are very large compared to the elastic strains, the results from a rigid-viscoplastic model are generally acceptable. Typically, solid, mechanics-based models use either a Lagrangian or an arbitrary Lagrangian Eulerian (ALE) approach utilizing remeshing capabilities [7]. These models are closer to the actual process since the material flow in FSW is essentially a solid flow and are especially useful in visualizing the final material deformation. However, on the downside these models are typically more expensive due to high computational time. The Eulerian formulations are usually computationally less expensive. An Eulerian formulation permits a fixed mesh and modeling of the steady-state FSW translating phase. The primary disadvantages of an Eulerian model include a lack of an elastic response and an inability to directly predict void formation [7]. The Eulerian formulation can be used in the finite element method as well as in the fluid, mechanics-based, constant-volume approach. Besides this, various mathematical modeling tools [15,16], simple geometrical models [17], and metalworking models [18] have also been developed.

In the CFD approach, the workpiece material is modeled as a viscous fluid with a strain rate and temperature dependent viscosity. Colegrove et al [4] used CFD to develop a two-dimensional model for material flow around the tool. They used local shear stresses

to govern the interface conditions in a 'slip' model. Torque, force, streamline and velocity vectors were determined using the model and validated with experiments. The model demonstrated the asymmetry in FSW as the deformation region in the advancing side was much smaller than the retreating side. A crucial finding of this model was that the material in the path of the pin was swept around the retreating side of the tool. The model however, used a uniform temperature field for the entire analysis. Smith et al [5] and Bendzsak et al [6] used the principles of fluid mechanics coupled with a thermo-mechanical model to develop a flow model. However, the heat input was modeled as viscous heating as opposed to frictional heating as this was a fluid-based model. This model included tool geometry, tool rotation speed, position and travel speed as inputs to predict the material flow profiles, process loads, and thermal profiles. It was indicated that three distinct flow regimes were formed below the tool shoulder, namely, (a) a region of rotation immediately below the shoulder where flow occurred in the direction of tool rotation, (b) a region where material is extruded past the rotating tool and this occurred towards the base of the pin, and (c) a region of transition between regions (a) and (b) where the flow had chaotic behavior.

Liechty et al [7] developed a three-dimensional Eulerian formulation for FSW which investigated two different contact conditions between the tool and the surrounding workpiece material. The constant velocity or 'sticking case' assumed that the velocity of the material around the tool was constant. However, the variable shear condition allowed material around the tool to slip with the shear stress on the material calculated as a function of the shear flow stress, the normal stress, the friction coefficient and the shear

friction factor. However, if the normal forces became too large, the relationship is converted to a Tresca friction law. The model also estimated the temperature field in the material using a variable heat flux equation which was a function of the variable shear stress mentioned earlier and the tool velocity. A comparison with experiments showed that the variable shear stress model had a better correlation than the constant velocity model. Also, interestingly, the variable shear stress model estimates that the maximum velocity of the material adjacent to the tool pin is only 9% of the rotational velocity of the tool.

There are several solid mechanics-based, numerical models of the FSW process which provide very insightful results. However, nearly all of them simulate either the welding stage or the dwell and the welding stages [8-14]. Zhang et al [8] developed a two-dimensional solid mechanics model using ABAQUS to investigate the flow and the residual stresses developed around the tool using tracer particles. Their model uses a rate independent elastic-plastic material. The effect of temperature on yielding is also considered. An interesting observation by Zhang et al [8] is that the material in the advancing side of the pin spins along with it a few times before sloughing off; however, the material in the retreating side does not spin with the pin. Askari et al [9] developed one of the earliest three-dimensional models using CTH, a code developed at Sandia National Lab. The model utilized the temperature and strain dependent Johnson-Cook material law to simulate temperature, strain and strain-rate. These models assumed a 'full stick - no slip' contact condition at the tool workpiece interface.

Ulysse [14] developed a three-dimensional, rigid, visco-plastic, finite-element model for analyzing the coupled thermo-mechanical state of FSW. In this model, 'some slip' is assumed at the contact interface and is prescribed as a tangential velocity field. Ulysse's model took into account the effects of tool feed rates and RPM settings in thick aluminum plates and helped to better model the friction stir welding process in three dimensions. Parametric studies were used in arriving at a combination of tool settings that promoted a good weld and avoided tool breakage from heat and shear stresses. A line of thermocouples was used to measure temperatures in the workpiece and develop isotherms. This work showed that increasing the feed rate resulted in an increase in shear force on the tool pin while increasing the RPMs reduced the shear force. Parametric tests have shown that welding parameters such as feed rate and RPMs can be modified to maximize welding effectiveness while avoiding stress concentrations that could cause the tool to fracture during a welding operation [14]. A good model would allow multiple simulations in the same amount of time and would help reduce the total amount of parametric testing needed. The common trend for all models discussed above is that the tool is in constant contact with the workpiece material.

Schmidt et al [12] developed an elastic-viscoplastic, thermomechanical model using ABAQUS/Explicit and the arbitrary Lagrangian Eulerian (ALE) formulation. This model sought to minimize the prescribed boundary conditions and the predefined fields. Notably, they did not predefine a boundary condition of a 'full stick state' between the tool and the workpiece material. The model results suggest that the development of a sticking condition at the tool-workpiece interface in the actual stir welding process is

important for the success of the material deposition process. A significant achievement of this model was that it could predict voids in the workpiece during material deposition. The model calculated a contact force when the slave surface (workpiece material) aligned to or penetrated the master surface (the analytically rigid tool) and predicted a void when there was either no contact or a negative contact. Their model shows that the heat generated along most of the contact surfaces is by plastic dissipation due to the presence of sticking condition in the majority of the area. A sliding condition exists along the outer periphery of the shoulder-workpiece interface. This region generates heat due to frictional dissipation. A similar contact approach has been used in the present dissertation. However, these models developed by Schmidt et al used a 'simplified plunge' wherein the simulation was started at the point where the shoulder already made contact with the work-piece.

While the simulations discussed above focus on the more common process parameters like tool speed and rotation speed, there is very little work on the effect of tool geometry as a process variable in FSW. Buffa et al [13] developed a fully coupled thermomechanical three-dimensional FEA model to study the effect of the pin angle on the FSW process. Their objective was to develop an effective methodology to optimally design weld tooling and process parameters for friction stir welding. A conical smooth pin was used and different tool designs were obtained by varying the taper angle of the conical pin and the pin and shoulder diameter. The workpiece was modeled as a rigid-viscoplastic material, which, as discussed earlier, produces acceptable results since the plastic strains in FSW are significantly larger than the elastic strains and the tool was

modeled as rigid. The commercial FEA code DEFORM 3D, was used in their research. Similar to the Schmidt model, they used a simplified plunge phase where the plunge was only 0.1 mm. They observed that increasing the pin angle produced a higher temperature in the weld zone and also produced a more uniform temperature distribution along the thickness which is likely to produce lesser distortion in the weld. Also, a larger pin angle produced significantly higher plastic deformation and strain rate until a certain limiting value beyond which the deformation and strain rate did not increase. They further demonstrated that a higher pin angle leads to a higher hydrostatic pressure in the weld region. However, a higher temperature and higher hydrostatic pressure also promote severe tool wear because both diffusion and abrasive wear, which are the main mechanisms in FSW welding tool wear, increase with temperature and hydrostatic pressure [13].

As is evident from the above discussions, there is a significant amount of research that has been done in understanding the material flow and temperature fields in FSW. However, a critical part of the process is the plunge stage of the weld. There is very little numerical simulation related work that is accomplished in this area. Goetz et al [19] developed a two-dimensional model using the commercial FEA code DEFORM to simulate the metal flow around the tool and the initial tool plunge in AA 1100 and Ti-6Al-4V. The research was directed towards predicting the tool and workpiece temperatures for various tool RPM and plunge rates. The material was modeled using a temperature, strain rate, strain and thermal conductivity dependent flow stress. From their studies it was evident that the flow stress almost doubled from the vicinity of the tool pin

to the outer edges of the localized metal flow region and this also coincided with the fact that the temperature around the pin was nearly 1.5 times higher than the temperature in the outer edges of the localized region. The tool plunge simulations were non-isothermal and axisymmetric. The tool and workpiece were assumed to be initially at room temperature. Loads and temperatures were determined for different tool RPM and plunge speeds. This study provided some interesting insights into the plunge region and also made an interesting case for further exploration with a three-dimensional model. Three-dimensional models involving the plunge phase have been developed for Friction Stir Spot Welding (FSSW) [20, 21]. Gerlich et al [20] used a computational fluid dynamics (CFD) approach to model FSSW with a plunge depth of 300 μm. On the other hand, Kakarla et al [21] used a solid mechanics approach to develop an isothermal model with a plunge depth of 317.5 μm. Guerdoux et al [22, 23] developed a numerical model of FSW using commercial codes FORGE3 and THERCAST. These models used the Norton-Hoff law as their material constitutive model as opposed to the Johnson-Cook law that is used in this research.

One of the more unique approaches to understanding material flow in FSW was suggested by Arbegast et al [18]. Based on the close similarity of microstructure and metal flow features of a friction stir weld to that of microstructure of a typical aluminum extrusion and forging, they suggested a metal-working model for FSW. The entire process was broken down into five conventional metal-working zones: (1) preheat, (2) initial deformation, (3) extrusion, (4) forging, and (5) post heat/cool down. In the pre-heat zone, the frictional heat generated during the tool's rotation and the adiabatic heating,

which is due to the material deformation, causes the temperature to rise ahead of the pin. The material thermal properties and the traverse and rotational speeds of the tool influence the heating of the zone. The influence of both the traverse speed and tool rotation on pre-heating was studied in detail by Mandal and Williamson [24] and Mandal [25]. According to Arbegast et al [18], an initial deformation zone forms when the material is heated above a critical temperature and the magnitude of stress exceeds the critical flow stress of the material, thus resulting in material flow. In this deformation zone, material is forced upwards close to the shoulder and also downwards where there is an extrusion zone. A small amount of material is also trapped in a vortex flow region under the tool pin in what they refer to as the swirl zone. This was also observed by flow simulation models developed by Nagathil et al [26]. An interesting theory is that there is a critical isotherm on the boundary of the extrusion zone beyond which there is no material flow as the temperature is below the critical limit and the magnitude of the stress is below the critical flow stress for the material. As the tool moves forward, a void is created immediately behind the pin. The material extruded out from the front of the tool fills this void. The tool shoulder contains the material in this zone and also applies a downward forging force hence it's named the forging zone. Material from the shoulder zone is dragged across the joint from the retreating side toward the advancing side. Beyond the forging zone is the 'cool down' zone. This is a simple yet effective material flow model which develops a relationship between the operating parameters, tool geometry and the material properties of the workpiece. The paper also claims that the predicted temperature, the width of the extrusion region and the extrusion pressure correlate well with the experimental data.

2.2 *Numerical simulation of FSW in steel*

Although there are several papers dealing with the numerical modeling of FSW in aluminum, very few deal with FSW of steels. One of the earliest works in this field was done by Zhu et al [27]. They proposed a three-dimensional thermal model for FSW of 304L steel. This model did not include flow during the welding process. The authors used a simulation called WELDSIM developed especially for the study of welding processes. Their main purpose was to investigate the variation of transient temperature and the residual stresses developed during the welding of steel. In this work, the authors used a process called an 'inverse' analysis as opposed to other works which used the numerical model to calculate the heat input. The temperature profiles were compared to an experiment and the heat input and the thermal coefficients were calculated so that the temperature profiles of the experiment and the model match. Based on the temperature field generated from this numerical model, the von Mises yield criterion and the associated flow rule were used to perform a thermo-mechanical analysis. The residual stresses were determined in a three-dimensional, elastic-plastic, mechanical simulation. Their experiments also show that only half of the total mechanical energy from the FSW machine is used in increasing the temperature of the steel workpiece as compared to about 75-80% in the case of aluminum. However, it was unclear if this was due to tool and workpiece material properties or due to possible errors in the numerical model [27]. Cho et al [28] developed a two-dimensional Eulerian formulation to model the temperature and flow around the tool pin in the case of stainless steel. The simplified Hart's model [29] was used as the constitutive material model for the simulation. Since the model was two dimensional, the vertical movement of material was not considered

and the focus was on material movement around the tool pin. Their results show that the temperatures are relatively low upstream of the tool and rise rapidly in the proximity of the pin. The isotherms exhibit a comet-like tail behind the tool. This is a standard pattern for nearly all moving heat sources. Also, both experiments and simulations performed by the authors indicate that the temperature on the advancing side is approximately 100°C higher than the retreating side.

Based on the previous two models on numerical simulations of FSW in steel, it was realized that a three-dimensional model incorporating both flow and temperature would be very useful in understanding the welding phase of FSW. Nandan et al [30] investigated the three-dimensional viscoplastic flow and heat transfer during the friction stir welding of mild steel both experimentally as well as numerically. Temperature-dependent thermal conductivity, specific heat and yield strength were considered. The computed results show that significant plastic flow occurs near the tool. The streamlines computed in the horizontal planes around the tool pin indicated an almost closed circular streamline suggesting a plug of material around the pin. The streamlines also suggested that the majority of the flow occurred on the retreating side.

2.3 *Previous studies on tool wear*

FSW tools are usually non-consumable in case of softer materials like aluminum alloys and copper; however, for harder materials like steel and manganese, consumption of the tool is a significant hindrance to the production of long welds with a consistent quality. Research carried out by Prado et al [31] at the University of Texas – El Paso

compared the tool wear rate during FSW of AA6061 and a metal matrix composite of AA6061 + 20% Al_2O_3. It was observed that although there was no significant tool wear during stir welding of AA6061, the tool wear for AA6061 + 20% Al_2O_3 was much higher for long welds. A comparison of wear rates was also made on the basis of tool rotational speed. It was observed that the wear rate increased until a speed of 1000 RPM and then decreased irregularly. The tool wear was larger towards the tip (away from the shoulder) due to plunging forces required to insert the tool in the workpiece. Since the heat generated in the stir welding process is highest around the shoulder region and decreases towards the tip, reduced wear in the regions of higher temperature could also explain this wear profile.

Although tool wear is a significant impediment in FSW of steel, there are very few publications on the mitigation of tool wear. In experiments conducted by Thomas et al [1,2], a pre-drilled hole, smaller than the diameter of the tool pin was machined into the workpiece prior to plunging the tool into the workpiece. The purpose of the pre-drilled hole was to reduce the high tool wear during plunging. In their research, Lienert et al [3] suggested that increased wear during plunging could be due to the high load spike which derives from the greater flow stress of the cold workpiece. Thomas et al [1,2] also allowed the tool to spin for a sufficient time period before initiating the traversing to plasticize the workpiece material in contact with the tool. These ongoing experiments reflect significant effort towards the development of a more robust friction stir welding technique for steel which offsets the problems with tool wear.

A few researchers have focused on finding tool materials, tool designs and processing strategies to extend tool life. While harder materials like carbides are being investigated, the criteria for selecting these materials are not well defined. For example, the metallurgical compatibility between tool material and the workpiece and their effects on the tool life is still not clearly understood [3]. The other factor to be considered in the development of new tool materials is the cost. Sterling et al [32] have successfully welded carbon manganese (C-Mn) steel with a polycrystalline cubic boron nitride (PCBN) tool material. However, due to the high temperatures encountered, they had to augment the tool with a cooling mechanism to prevent excessive heating of the spindle bearings of the stir welding machine. The inclusion of a cooling mechanism added to the cost of using expensive tool materials and significantly increased the cost of the entire process.

An alternative approach would be to pre-heat the workpiece. A pre-heating source would possibly soften the material and thus reduce the amount of frictional heat required to be generated by the tool for stir welding. This reduced demand on frictional heat would in turn decrease the required rotational speeds and subsequently the wear rate. This approach has been suggested by several researchers [1-3, 24, 25]. Approaches for pre-heating could range from just pre-heating the plunge region of the workpiece to continuous heating throughout the welding process. In the majority of cases, pre-heating techniques involve flame heating, induction or resistance heating, arc/plasma heating or laser-assisted heating. Evidence from previous research suggests that pre-heating may have other added benefits apart from decreasing tool wear. For example, Krishnan's [33]

experiments showed that stir welding is essentially an extrusion process, and material ahead of the tool is heated by friction and moved behind it. This means that there is a cavity behind the tool, which can be filled with air and result in oxidation. He also proposed that a lesser time of contact with the air could possibly reduce oxidation. An additional heat source ahead of the tool would expedite the extrusion process and subsequently reduce the time of contact with air and thus reduce the amount of oxidation during the welding process. Mandal and Williamson [24] and Mandal [25] proposed a thermomechanical hot channel coupled to a FSW process. Their idea was to form a thermo-mechanical hot channel ahead of the stir-welding tool which would reduce the heat required to be generated by the stir tool, which in turn would reduce the required rotational speed, and hence the wear rate. The concept is shown in Fig. 2-1 [24, 25]. A similar approach had been used earlier by Kannatey-Asibu [34] for reducing the thermal gradient and hence distortions in laser welding. The emphasis of Mandal [25] was on the integration of a friction stir welding process with suitable pre-heating sources to create a thermomechanical hot channel. The concept was demonstrated as an analytical solution based on the Rosenthal [35] model for thermal distribution during welding. The analytical solution assumed that the FSW tool and the pre-heating sources were moving point heat sources. Only the heat input from friction was considered. Feng et al [36] had developed an equation for the heat input from the tool, which assumed that the heat is generated by a line contact between the tool shoulder's rim and the workpiece, which is fairly accurate as long the shoulder stays in contact with the workpiece. The heat generated is given by,

$$Q = \int_0^{2\pi} \mu F \omega \, r \, d\alpha = 2\pi \mu F \omega r \qquad (2.1)$$

where F is the downward force applied by the tool on the workpiece

ω is the angular velocity of rotation of tool

μ is the coefficient of friction between the tool and the workpiece

r is the radius of the tool shoulder

The model of Mandal [25] demonstrated that the temperature ahead of the tool when using a pre-heating approach could be significantly higher than that of a regular stir weld which would soften the material and reduce tool wear. This could also possibly increase welding speeds and result in a decrease in production costs. However, this approach was developed for mitigation of tool wear during the welding phase of FSW. The current research focuses on reducing wear during the plunge stage, a phase during which the majority of tool wear occurs.

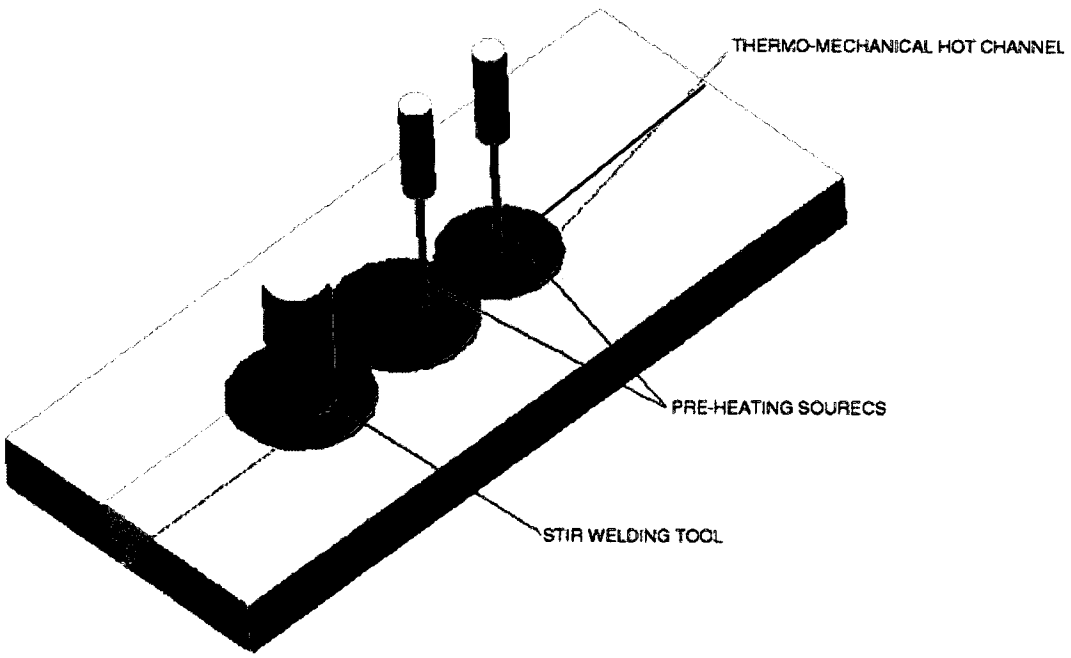

Fig. 2-1 Schematic of a FSW process coupled to pre-heating sources [24]

References

1. Thomas, W., "Friction Stir Welding of Ferrous Materials; A Feasibility Study" *Proceedings of First International Symposium on Friction Stir Welding,* Thousand Oaks, California, 14-16 June 1999.

2. Thomas, W., 1999, "Feasibility of Friction Stir Welding Steel" *Science and Technology of welding and joining,* Vol. 4, pp. 365-372.

3. Lienert T.J., Stellwag W.L. Jr., Grimmett, B.B. and Warke, R.W., 2003 "Friction stir welding studies on mild steel" *Supplement to the Welding Journal*, pp.1s-9s.

4. Colegrove P., Shercliff, H., 2003, "2-Dimensional CFD modeling of flow round profiled FSW tooling" *Friction Stir Welding and Processing II,* TMS, pp.13-22

5. Smith, C.B., Bendzsak, G.B., North, T.H., Hinrichs, J.F., Noruk, J.S., Heideman, R.J., *Ninth International Conference on Computer Technology in Welding*, Detroit, Michigan, 28–30 September, 1999, pp. 475.

6. Bendzsak, G.J., Smith, C.B., *Proceedings of the Second International Symposium on Friction Stir Welding*, Gothenburg, Sweden, June 26–28, 2000.

7. Liechty, B.C., Webb, B.W., "Modeling the frictional boundary condition in friction stir welding" *International Journal of Machine Tools & Manufacture*, 2008, pp. 1474-1485.

8. Zhang H.W., Zhang, Z., Chen, J.T., 2005, "The finite element simulation of the friction stir welding process" *Materials Science and Engineering A*, pp.340–348.

9. Askari, A., Silling, S., London, B., Mahoney, M., 2001, "Modeling and Analysis of Friction StirWelding Processes" *Friction Stir Welding and Processing*, pp. 43-54.

10. Schmidt, H., Hattel, J., Wert, J., 2004, "An analytical model for heat generation in friction stir welding" *Modeling and Simulation in Materials Science and Engineering*, pp. 143-157.

11. Schmidt, H., Hattel, J., "Modelling thermomechanical conditions at the tool/matrix interface in Friction Stir Welding" *Proceedings of the 5th International Friction Stir Welding Symposium*, Metz, France, 14-16 September, 2004.

12. Schmidt, H., Hattel, J., Wert, J., 2005, "A local model for the thermomechanical conditions in friction stir welding" *Modeling and Simulation in Materials Science and Engineering*, pp. 77-93.

13. Buffa, G., Hua, J., Shivpuri, R., Fratini, L., 2006, "Design of the friction stir welding tool using the continuum based FEM model" *Materials Science and Engineering A*, pp. 381-388.

14. Ulysse, P., 2002, "Three-dimensional modeling of the friction stir welding process" *International Journal of Machine Tools and Manufacture*, pp. 1549-1557.

15. Stewart, M.B., Adamas, G.P., Nunes Jr., A.C., Romine, P., 1998 "A combined experimental and analytical modeling approach to understanding friction stir welding" *Developments in Theoretical and Applied Mechanics*, pp. 472–484.

16. Nunes Jr., A.C., "Wiping metal transfer in friction stir welding" *Aluminum 2001*, New Orleans, LA, February 11-15, 2001, pp. 235-248.

17. Ke, L., Xing, L., Indacochea, J.E., *Joining of Advanced and Specialty Materials IV*, "The materials flow pattern and model in the friction stir welding of aluminum alloy" Indianapolis, Indiana, November 5-8, 2001, pp. 125–134.

18. Arbegast, W.J., "Modeling friction stir joining as a metalworking process" *Hot Deformation of Aluminum Alloys III*, San Diego, CA, March 3-6, 2003, pp. 313-318.

19. Goetz, R.L., Jata, K.V., "Modeling friction stir welding of titanium and aluminum alloys" *Friction Stir Welding and Processing*, TMS, 2001, pp. 35-42.

20. Gerlich, A., Su, P., Bendzsak, G.J., North, T.H., "Numerical modeling of FSW spot welding: preliminary results" *Friction Stir Welding and Processing III*, TMS, 2005.

21. Kakarla, S.T., Muci-Kuchler, K.H., Arbegast, W.J., Allen, C.D., "Three dimensional finite element model of the friction stir spot welding process" *Friction Stir Welding and Processing III*, TMS, 2005.

22. Guerdoux, S., Miles, M., Fourment, L., Sorensen, C., "Numerical simulation of the friction stir welding process using both Lagrangian and arbitrary Lagrangian Eulerian formulations" *8th International Conference on Numerical Methods in Industrial Forming Process (NUMIFOM)*, 2004.

23. Guerdoux, S., Fourment, L., Nelson, T., Miles, M., Sorensen, C., "Numerical simulation of the friction stir welding process using Lagrangian, Eulerian and ALE approaches" *8th International Conference on Computational Plasticity*, Barcelona, September 5-7, 2005.

24. Mandal, S., Williamson, K., 2006, "A thermomechanical hot channel approach for friction stir welding" *Journal of Materials Processing Technology*, pp.190-194.

25. Mandal, S., "Analytical model of a thermomechanical hot channel coupled to a friction stir welding process" *M.S. Thesis*, 2003, Old Dominion University.

26. Nagathil, R., Hou, G., Demuren, A. "Modeling experience on friction stir welding using FLUENT" *SAE World Congress*, Detroit, MI, April 11-14, 2005.

27. Zhu, X.K., Chao, Y.J., 2005, "Numerical simulation of transient temperature and residual stresses in friction stir welding of 304L stainless steel" *Journal of Materials Processing Technology*, pp. 263-272.

28. Cho, J-H., Boyce, D.E., Dawson, P.R., 2005, "Modeling strain hardening and texture evolution in friction stir welding of stainless steel" *Materials Science and Engineering A*, pp. 146-163.

29. Hart, E. W., 1976, "Constitutive relations for the non-elastic deformation of metals" *Transactions of ASME: Journal of Engineering Materials Technology*, pp.193-202.

30. Nandan, R., Roy, G.G., Lienert, T.J., Debroy, T., 2007, "Three-dimensional heat and material flow during friction stir welding of mild steel" *Acta Materialia*, pp. 883-895.

31. Prado, R.A., Murr, L.E., Shindo, D.J. and Soto, K.F., 2001 "Tool wear in friction stir welding of aluminum alloy 6061 + 20% Al_2O_3: A Preliminary Study" *Scripta Materiala*, pp. 75-80.

32. Sterling, C.J., Nelson, T.W., Sorensen, C.D., Steel, R.J., Packer, S.M., "Friction Stir Welding of Quenched and Tempered C-Mn Steel" *Proceedings of Friction Stir Welding and Processing II*, 2003, pp. 165-171.

33. Krishnan, K.N., 2002, "On the Formation of Onion Rings in Friction Stir Welds" *Materials Science and Engineering A*, pp. 246-251.

34. Kannatey-Asibu, Jr., Elijah, 1991, "Thermal Aspects of Split-beam Laser Welding Concept" *Journal of Engineering Materials and Technology*, pp. 215-221.

35. Rosenthal, D., 1941 "Mathematical Theory of Heat Distribution During Welding and Cutting" *Welding Journal*, pp. 20-25.

36. Feng, Z., Gould, J.E., Lienert, T.J., 1998, "A Heat Flow Model for Friction Stir Welding of Steel" *Proceedings of Hot Deformation of Aluminum Alloys*, pp 149-158, TMS.

Chapter 3

NUMERICAL SIMULATION OF PLUNGE IN FSW

The numerical modeling of FSW poses a challenge due to high strain rates and temperatures involved in the process resulting in a complicated problem involving, non-linear material behavior. Simulation of the entire process was performed using an elasto-plastic constitutive law available in ABAQUS finite element code. ABAQUS is used due to its strong capabilities of handling non-linear problems and the built-in Johnson-Cook material law which is used in the present problem. The use of remeshing is available in the ABAQUS explicit solver using the arbitrary Lagrangian Eulerian (ALE) approach. This is crucial to eliminate excessive element distortion which could lead to premature termination of the problem in cases involving large deformations.

The model consists of a deformable workpiece and a rigid stir welding tool. The workpiece is meshed using 8 node coupled temperature displacement, brick elements (C3D8RT). The mesh is graded in a way such that there is a higher mesh density around the tool plunge area. This improves the accuracy of the solution around the tool without tremendously increasing the computational time. The graded meshes are obtained by partitioning the workpiece into smaller cells. Different mesh densities were tried out before arriving at the final model. The final mesh is shown in Fig. 3-1 [1,2]. The tool dimensions used in the model are shown in Fig. 3-2. In order to simplify the FEM, the tool pin has been modeled as a straight cylindrical pin as opposed to the various

complicated geometries that are sometimes used in experiments. The influence of various pin geometries on friction stir processing of 2000 and 6000 series aluminum has been experimentally studied by Elangovan et al [3, 4]. The concave shoulder geometry used in this simulation is a popular tool design with the cavity providing a means to prevent the removal of plasticized material from under the shoulder [5]. The use of fillets to reduce stress concentration and increase surface contact area is also very common [5]. The workpiece is constrained at the bottom surface to prevent the bending of the surface and the sides are constrained such that there is no deformation along the boundary other than compression along the tool plunge direction. The tool is modeled as a rigid surface with no thermal degrees of freedom. For the contact conditions between the tool and the workpiece, the tool is modeled as a master surface and the workpiece as a slave. A constant friction coefficient of 0.3 is assumed between the tool and the workpiece [6] and the penalty contact method is used to model the contact interaction between the two surfaces. The tool rotational speed is set at 300 RPM and the tool plunge velocity is set to a uniform value of 4 mm/s.

3.1 *Material Law*

The selection of an appropriate constitutive law to reflect the interaction of flow stress with temperature, plastic strain and strain rate is essential for modeling the FSW process. For this reason the temperature and strain rate dependent elastic-plastic Johnson-Cook law is selected for this model. Schmidt et al [5] have also previously used this model successfully to simulate FSW. The constitutive law in this case calculates the flow stress as a function of temperature and strain rate up to the melting point or solidus

temperature. The material selected for this simulation is AA 2024. The availability of the Johnson-Cook parameters and the frequent application of FSW to weld AA 2024 make this a good candidate material for the simulation. The alloy composition is shown in Table 3.1.The solidus temperature for AA 2024 is set to 502°C. The Johnson-Cook constitutive law is given by [7,8]:

$$\bar{\sigma} = \left[A + B\left(\bar{\varepsilon}^{pl}\right)^{n}\right]\left[1 + C\ln\left(\frac{\dot{\bar{\varepsilon}}^{pl}}{\dot{\varepsilon}_0}\right)\right]\left(1 - \hat{\theta}^{m}\right), \tag{3.1}$$

$\hat{\theta}$ is the nondimensional temperature defined as

$$\hat{\theta} \equiv \begin{cases} 0 & for \quad \theta < \theta_{transition} \\ \left(\theta - \theta_{transition}\right) / \left(\theta_{melt} - \theta_{transition}\right) & for \quad \theta_{transition} \le \theta \le \theta_{melt} \\ 1 & for \quad \theta > \theta_{melt} \end{cases}, \tag{3.2}$$

Johnson-Cook strain rate dependence assumes that [7,8]

$$\bar{\sigma} = \sigma^{0}\left(\bar{\varepsilon}^{pl}, \theta\right) R\left(\dot{\bar{\varepsilon}}^{pl}\right), \tag{3.3}$$

and

$$\dot{\bar{\varepsilon}}^{pl} = \dot{\varepsilon}_0 \exp\left[\frac{1}{C}(R-1)\right] \qquad for \qquad \bar{\sigma} \ge \sigma^{0}, \tag{3.4}$$

where

$\bar{\sigma}$ is the yield stress at nonzero strain rate;

$\dot{\bar{\varepsilon}}^{pl}$ is the equivalent plastic strain rate;

$\dot{\varepsilon}_0$ and C are material parameters measured at or below the transition temperature, $\theta_{transition}$;

$\sigma^0(\bar{\varepsilon}^{pl}, \theta)$ is the static yield stress; and

$R(\dot{\bar{\varepsilon}}^{pl})$ is the ratio of the yield stress at nonzero strain rate to the static yield stress (so that $R(\dot{\varepsilon}_0) = 1.0$).

A, B, C, n, m are material parameters that are measured at or below the transition temperature.

These material parameters for AA 2024-T3 are adapted from Lesuer [9] and Schmidt et al [5] and are shown in Table 3.2. Other thermal and mechanical properties used in this model are listed in Table 3.3.

3.2 *Results and Discussion*

The tool was plunged into a 100mm x 100mm x 20mm AA 2024-T3 for a period of 3 sec up to a distance of 11 mm. The primary challenge in this simulation was the premature termination of the solution due to excessive element distortion. The Arbitrary Lagrangian Eulerian (ALE) feature was engaged to reduce excessive element distortion and to constantly generate remeshing. However, this did not resolve the issue of element distortion. It was anticipated that increasing the frequency of remeshing and increasing the mesh sweeps per increment would minimize if not completely eliminate the excessive element distortion, but neither materialized. The next approach was to remove the

elements which were excessively distorted from the calculation, thus preventing a premature termination. This was achieved using the 'shear failure' criterion built into ABAQUS/Explicit. This method has been previously used in ABAQUS based finite element modeling of machining problems [11]. In this method, an element that reaches a pre-set damage threshold is automatically deleted. The pre-set damage threshold is based on the Johnson-Cook shear failure criterion. However, using the Johnson-Cook shear failure criteria resulted in too many elements being deleted from the original model, thus creating large voids. This was probably due to the fact that the parameters for the Johnson-Cook shear failure criterion were designed for ballistic purposes [9] which involve higher strain rates compared to the strain rates involved in FSW. Finally, a pure Lagrangian approach was adopted for the simulation and this resulted in solution convergence without premature termination due to excessive element distortion. Using these initial parameters in the FEM model, different mesh densities were investigated. Normally, a higher mesh density provides for higher accuracy but also increases the computational time, therefore, a trade-off between time and accuracy becomes crucial. In this case, four different mesh densities were investigated. The workpiece was initially meshed with 1600 elements with a higher mesh density closer to the tool and with a similar distribution that was maintained right along the thickness. In the subsequent models, the workpiece was partitioned half way along the thickness and a higher mesh density was used on the upper half close to the penetration area. This provided a much higher mesh density around the tool without a huge increase in computation time. The three models meshed using this method had 2400, 2904 and 3388 elements. Higher mesh densities were investigated with 4032 elements but a successful convergent solution was

never reached. The model with 3388 elements resulted in a solution that correlated well with the experimental results; therefore, it was decided to adopt the model with 3388 elements in this research.

Fig. 3-3 shows the temperature distribution in the AA 2024 workpiece at the end of the plunge period [1,2]. As expected, the temperatures are comparatively higher at the trailing edge. The temperature history shown in Fig. 3-4 was recorded at the tool tip for the entire duration of the plunge and was compared with experimental data obtained from Gerlich et al [12]. They measured the temperature at the tool tip during a plunge into AA 6111. The temperature history correlated well with the experimental data in all of the four models with different mesh densities and particularly in the models having 2904 and 3388 elements. The minor differences between the current simulation results and the experimental measurements of Gerlich et al [12] could be attributed to the slightly different materials used for the simulation and the experiment, AA 2024 and AA 6111 alloys respectively. A difference in hardening properties in the two materials around that temperature range could make a difference in the measured temperature values. Fig. 3-5 shows the axial force on the tool as a function of time. As is evident from the graph, the axial force calculated from the ABAQUS simulation does not correlate as well with the experimental data as the temperature does. It is noted that as the mesh density is increased, the peak loads on the tool approach the experimental data results obtained from the literature [12]. Interestingly, both the numerical simulation and the experimental data from Gerlich et al [12] behave similarly as the loads seem to rise until a little after 1 sec and then slightly drop before rising back up again. A plausible explanation for this

behavior could be the high axial forces experienced during plunging into a relatively cold metal with significantly high flow stresses and hardness. As the workpiece slightly heats up, the load drops and then rises again with an increase in the plunge depth. A similar trend was observed by Santella et al [13] in their plunge experiments on AA 6061 + 20% wt Al_2O_3. Gerlich et al [12] suggest that this temporary drop could be due to a possible localized melting in the region underneath the tool.

The energies involved in the process have been plotted with respect to time in Fig. 3-6 [2]. The energy balance in the model is represented by the following equation [19].

$$ETOTAL = ALLWK - ALLFD - ALLIE \quad (3.5)$$

where *ALLWK* is the external work into the system, *ALLFD* is the energy dissipated by friction, and *ALLIE* is the internal energy which is equivalent to the summation of plastic energy (*ALLPD*) and the artificial energy (*ALLAE*). The artificial energy in the model is the energy produced due to the application of hourglass control, which prevents excessive distortion in the mesh. In this case, the relaxed stiffness hourglass control method was used. It can be seen from Fig. 3-6 that the artificial energy is a reasonably small percentage of the total internal energy (*ALLIE*), which is desirable. This energy can be further reduced by improving the mesh density. From Fig. 3-6, it can also be seen that at the start of the process nearly all of the input work (*ALLWK*) is dissipated away as friction (*ALLFD*). However, as the process advances, plastic dissipation (*ALLPD*) steadily rises. This is consistent with Schmidt et al [6] who propose that most of the heat generated in the plunge phase is due to frictional dissipation. It is very likely that as the energy dissipated by the plastic work increases, the tool wear decreases because the

thermomechanical conditions can be maintained by the heat generated from plastic dissipation as opposed to that from friction.

3.3 *Summary*

In this chapter a numerical investigation was performed on the plunge stage of friction stir welding. This is a vital phase as it generates the initial thermomechanical conditions in the material. ABAQUS was used to generate a numerical model with the strain-rate and temperature dependent Johnson-Cook law as the material constitutive law. The simulations were compared with experimental results obtained from literature. The temperature calculated from the model provided excellent correlation with the experimental data from the literature. However, the axial forces from the experiment and simulation do not correlate as closely as the temperature. This could be further improved by a finer mesh, which could also possibly lead to a higher computational cost. In a subsequent chapter, the results are compared with experiments performed during the course of this research and the model was found to have good correlation with experiments. This research is a significant step in the direction of the study of thermomechanical conditions in the plunge area and forms the foundation for the development of the donor material concept to reduce tool wear.

Al	Cu	Mg	Mn	Other
94.7%	3.8%	1.2%	0.3%	Trace

Table 3.1 Alloy composition of AA 2024-T3 [14]

A	369 MPa
B	684 MPa
C	0.0083
n	0.73
m	1.7

Table 3.2 Johnson-Cook parameters for AA 2024-T3 [6,9]

Thermal Conductivity	121 W/m-K
Specific Heat	875 J/kg-^{o}C
Elastic Modulus	73 GPa
Poisson's Ratio	0.34
Density	2770 kg/m^{3}

Table 3.3 Material Properties of Al 2024-T3 used in plunge model [10,14]

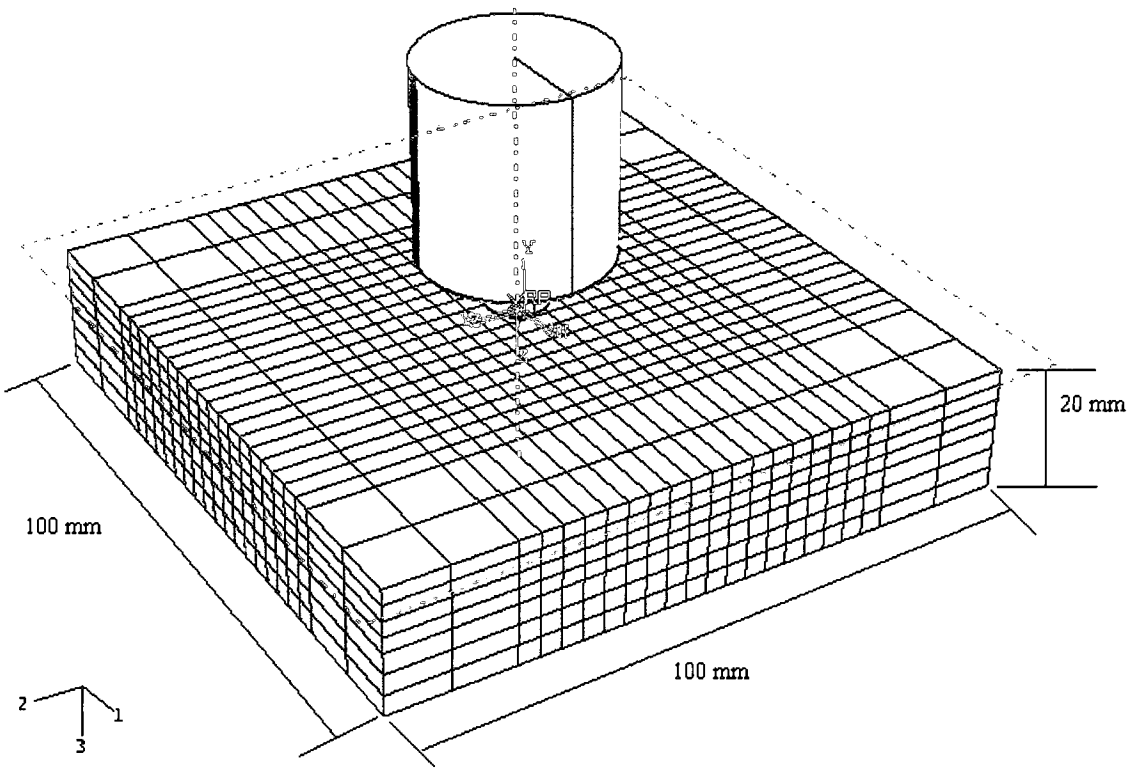

Fig. 3-1 Final mesh for plunge simulation [1,2]

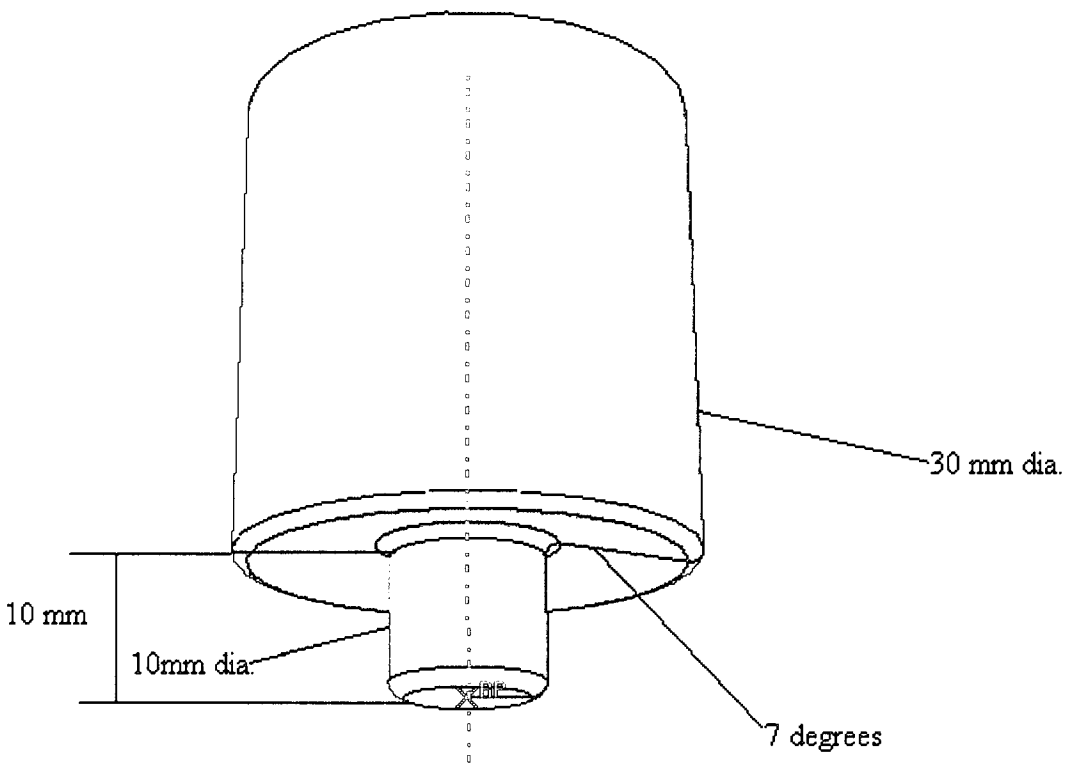

Fig. 3-2 Tool design for simulation [1,2]

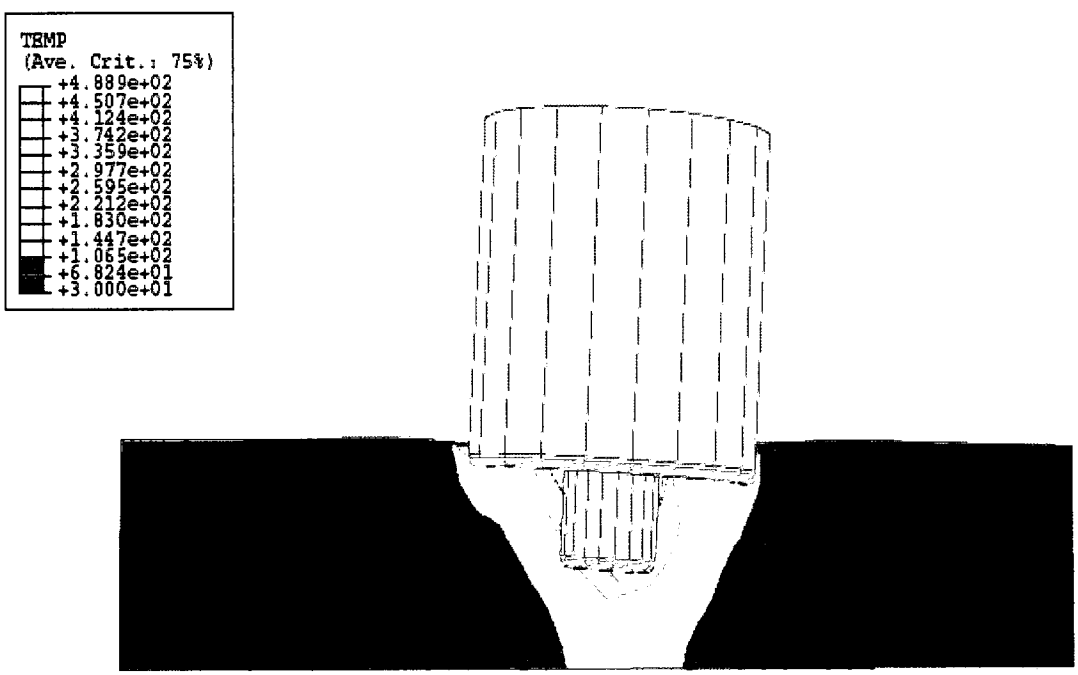

Fig. 3-3 Temperature distribution in aluminum 2024-T3 at the end of a 3 sec plunge [1,2]

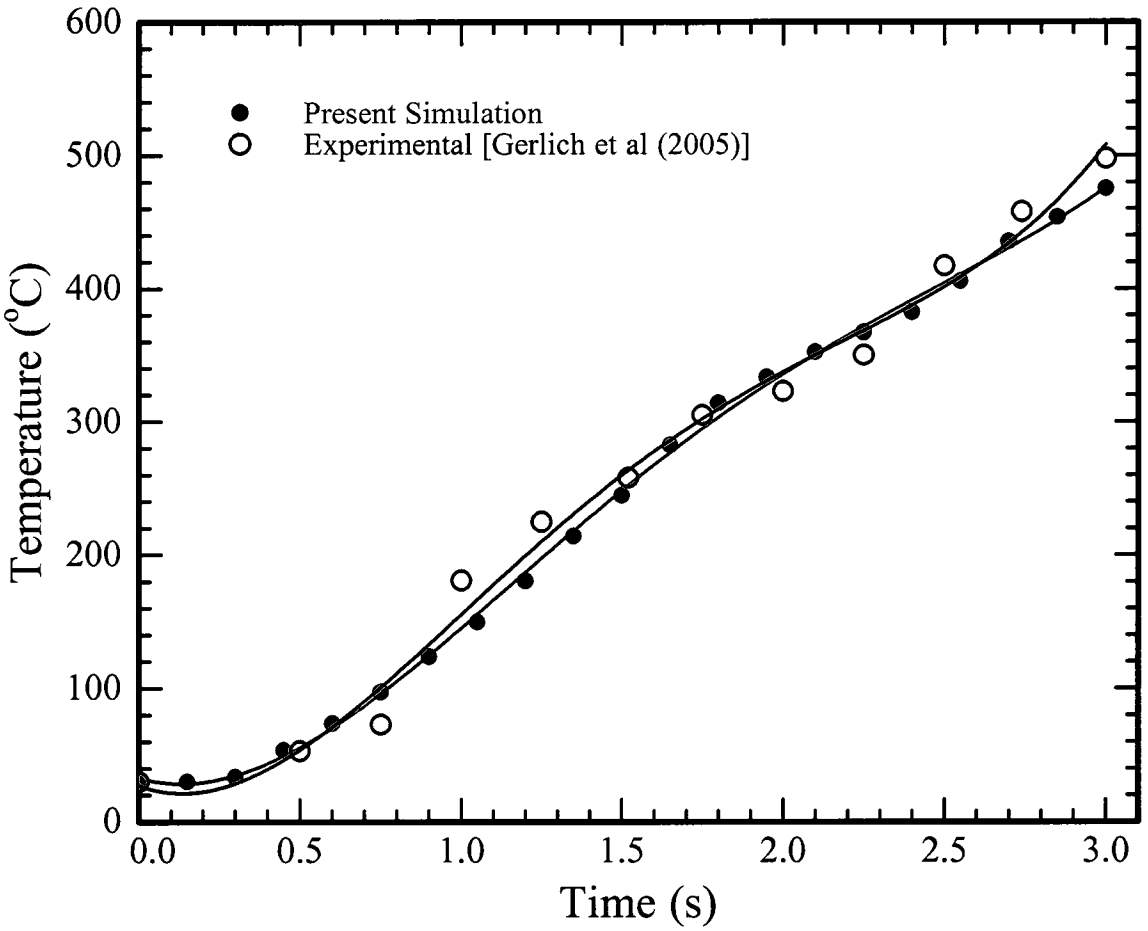

Fig. 3-4 Comparison of temperature at tool tip [1,2]

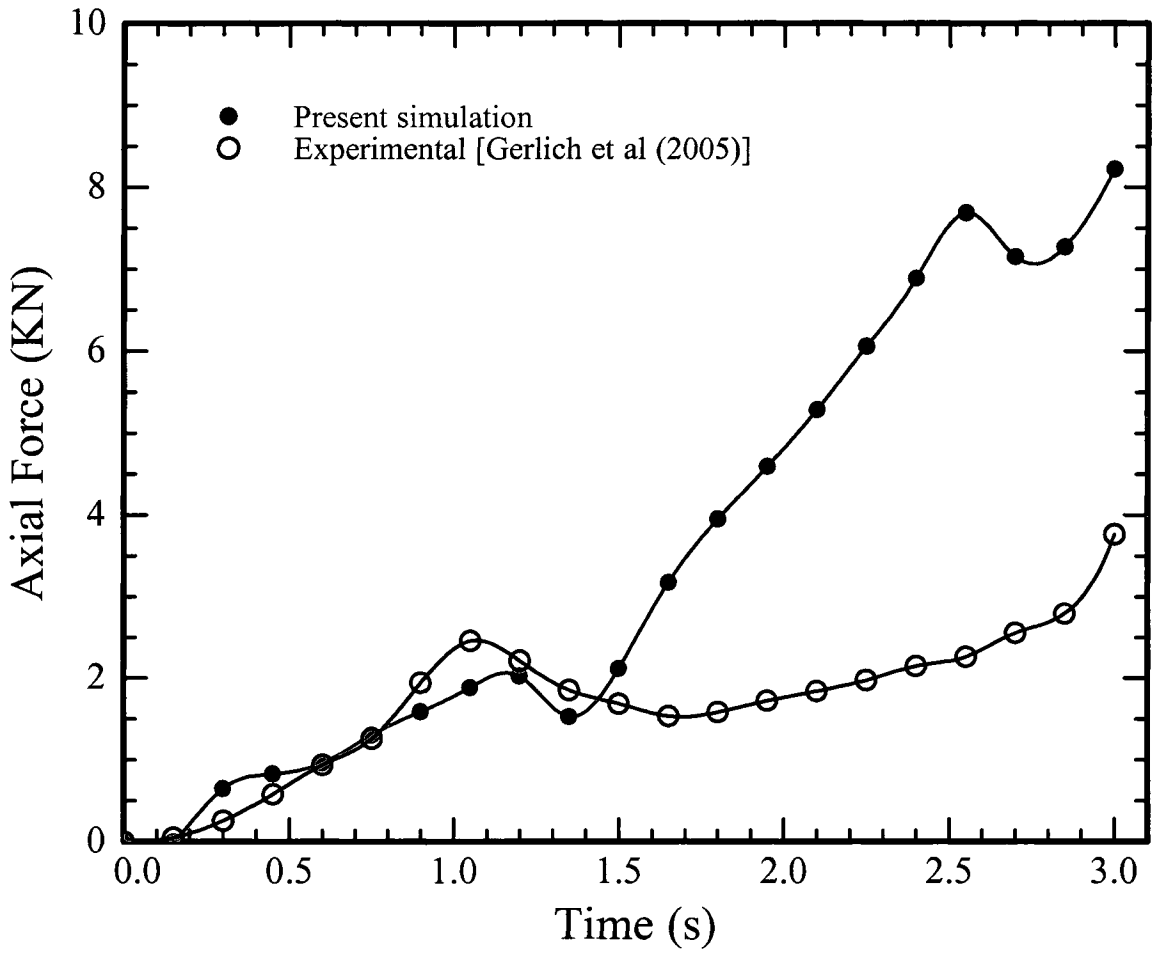

Fig. 3-5 Axial force comparison with experimental data from Gerlich et al (2005) [1,2]

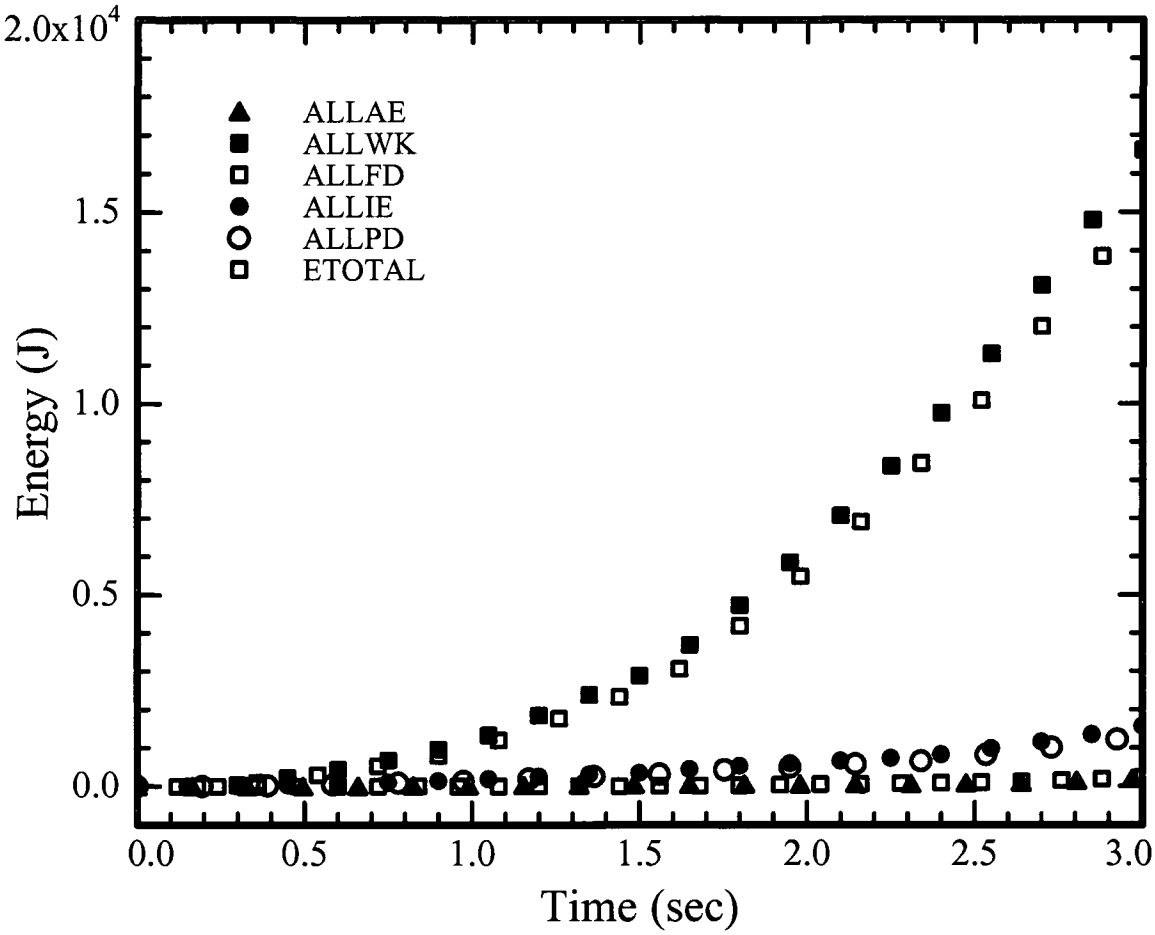

Fig. 3-6 Energy in present ABAQUS simulation [2]

References

1. Mandal, S., Rice, J., Elmustafa, A.A., "A numerical study of the plunge stage in friction stir welding using ABAQUS," *Friction Stir Welding and Processing IV*, 2007, pp. 127-133.

2. Mandal, S., Rice, J., Elmustafa, A.A., 2008, "Experimental and numerical investigation of the plunge stage in friction stir welding" *Journal of Materials Processing Technology*, pp. 411-419.

3. Elangovan, K., Balasubramanian, V., 2007, "Influences of pin profile and rotational speed of the tool on the formation of friction stir processing zone in AA2219 aluminum alloy" *Materials Science and Engineering A*, pp. 7-18.

4. Elangovan, K., Balasubramanian, V., 2007, "Influences of tool pin profile and tool shoulder diameter on the formation of friction stir processing zone in AA6061 aluminum alloy" *Materials and Design*, pp. 362-373.

5. Scialpi, A., De Filippis, L.A.C., Cavaliere, P., 2006, "Influence of shoulder geometries on microstructure and mechanical properties of friction stir welded 6082 aluminum alloys" *Materials and Design*, pp. 1124-1129.

6. Schmidt, H., Hattel, J., Wert, J., 2005, "A local model for the thermomechanical conditions in friction stir welding" *Modeling and Simulation in Materials Science and Engineering*, pp. 77-93.

7. ABAQUS Version 6.5 Documentation, Hibbit Karlson and Sorensen Inc., 2004.

8. Johnson, G. R., Cook, W. H., 1985, "Fracture characteristics of three metals subjected to various strains, strain rates, temperatures and pressures," *Engineering Fracture Mechanics*, pp. 31-48.

9. Lesuer, D.R., "Experimental investigations of material models for Ti-6Al-4V Titanium and 2024-T3 Aluminum" *DOT/FAA/AR-00/25*, 2000.

10. Metals Handbook, 10th Edition, ASM International, 1990.

11. Wen, Q., Guo,Y.B., Todd, B.A., 2006, "An adaptive FEA method to predict surface quality in hard machining" *Journal of Materials Processing Technology*, pp. 21-28.

12. Gerlich, A., Su, P., Bendzsak, G.J., North, T.H., 2005, "Tool penetration during friction stir spot welding of Al and Mg alloys" *Journal of Materials Science*, pp. 6473–6481.

13. Santella, M., "Plunge testing to evaluate tool materials for friction stir welding of 6061+20wt% Al_2O_3 composite" *4th International Friction Stir Symposium,* Park City, Utah, 2003.

14. Retrieved material properties April 15, 2009 from http://www.matweb.com

Chapter 4

FSW PLUNGE EXPERIMENTS

Although a significant portion of this research focuses on FEA-based simulation of the plunge process, it is very essential that these simulations are backed by at least preliminary experiments. This becomes extremely critical as the issues experienced during experiments are very often different from those experienced during simulation. An understanding of both of these research tools helps to develop a better understanding of the process. This chapter documents the plunge experiments performed on AA 2024. During the experiment, the axial load in the process and the temperatures generated in the workpiece material were recorded. The challenges faced during the experiments are also discussed. A comparison between the experiments and simulation is also discussed to gather a better perspective.

4.1 *Experimental Equipment*

The experimental set up is shown in Fig. 4-1 [1]. The experiments were carried out on a Cincinnati-Greaves milling machine modified to perform friction stir welding. The machine had a spindle rotational speed ranging from 80 RPM to 2720 RPM and the feed rate of the milling table ranged from 9/16 in/min to 9 3/16 in/min. The machine was retrofitted with a 10 HP motor which was sufficient to weld high strength grades of aluminum and copper but the machine is not suited to weld high hardness materials like manganese and steel. In an effort to better understand the plunge phase of FSW, it was crucial to measure axial forces. To be able to do this with a fairly old milling machine was a challenging task and to do it economically considering the limited resources

complicated the job even further. Several options were considered including using four miniature 'donut' load cells which would be placed between the base plate and the machine table around the four bolts that clamp down the base plate. This appeared to be a feasible solution. However, it was expensive because it requires four separate load cells. Also, the Data Acquisition System (DAQ) card used in this experiment could not handle read outs from four separate channels. Finally the machine was altered according to a setup designed by Mitchell et al [2] and modified by Henderson [3] to enable load measurement capabilities. The setup is shown in the schematic diagram of Fig. 4-2. A miniature button type load cell was placed in a plastic sleeve and positioned inside the machine arbor in such a way that it was always in contact with the tool. The machine's regular draw bar was replaced with a hollow drawbar. The load cell wires were passed through this hollow drawbar to a rotating electrical connector (REC) at the top of the machine head, which operates similar to a slip ring. The top of the REC was clamped tightly to the machine. This permits the bottom half of the connector, which is attached to the wires, to spin with the machine spindle at high speeds while the top part remained stationary. Data cables connected to the top transferred data from the load cell to the DAQ. The DAQ used for the experiments was a National Instruments PCI 6024E card. LabView was used to read out and store the data from the DAQ.

A backing plate measuring 16" x 10" x 1.5", and made of low-carbon steel, was designed to support the specimens to be welded. Recessed holes were machined onto the plate to fit in T-slot bolts to clamp the plate to the milling machine table. The plate's bottom contained machined ribs to allow for alignment with respect to the milling

machine table. The plate was designed to provide lateral clamping force by having bars bolted to both sides of the plate between which the specimen is placed. Downward clamping force was obtained by placing a large bar on top of the specimen on either side. These bars were bolted down to the backing plate. This ensured that the specimen was completely constrained during the welding process. For the plunge experiments, the specimens were clamped on a vise grip bolted down to the machine table.

4.2 *Experimental Setup*

Plunge experiments were performed on AA 2024 coupons of dimensions 38.1mm x 38.1mm x 12.5mm thick. The experimental setup is shown in Fig. 4-1. The plunges were made using a H-13 steel tool heat treated to a hardness of R_c 46 to 48. The axial load on the tool and temperatures around the tool pin were measured during the experiments. The temperature was measured using glass insulated Omega 20 gauge K-type thermocouples. The thermocouples were positioned 2 mm away from the pin and 6.5 mm from the top surface of the workpiece through 2 mm diameter holes. The thermocouples were placed at similar positions at the leading and trailing side. The thermocouples and the load cell were connected to the DAQ using a 50 channel connector board. The temperature data from the thermocouples were converted to a milliVolt (mV) output based on the calibration charts from Omega, to make data operations easier since the output data from the load cell was also in mV.

The experiments were performed by penetrating the tool into the workpiece till the tool shoulders made contact with the workpiece. The tool was then allowed to spin

without moving forward. The machine was only capable of manual plunge, which resulted in different plunge times during each run. Additionally, due to the fact that the machine is manually operated, the plunge rates during these experiments were much lower than the plunge rates in the simulation discussed earlier and the experiments conducted by Gerlich et al [4]. This led to different results in terms of temperature and axial load. The approximate average speed was estimated to be 0.45 mm/sec. The plunges took around 14 secs to complete and then the dwell period was estimated to be 45 secs. A significantly long period of dwell was added at the end of the plunge to observe if a steady state condition could be attained for the axial load on the tool and temperature in the tool's vicinity. All the plunges were made with the milling machine head set at a 3^{o} angle.

4.3 *Experimental Results*

Fig. 4-3 shows the variation of axial load (kN) with time (sec). The plunge was completed in 14 sec and the tool was then allowed to dwell for 45 secs prior to retraction. The peak load of approximately 25 kN was observed at the 5 sec mark. At the end of the plunge of 14 secs, the load dropped to approximately 8 kN where it remained fairly steady until the end of the dwell period. It can be seen from the figure that the peak load occurred prior to the completion of the plunge. This can possibly be attributed to the slow plunge speed, which provided enough time to the material underneath the tool to heat up by conduction, and then soften it which resulted in lower axial loads.

Fig. 4-4 shows the variation of temperature (°C) with time (sec) at the trailing and leading edges. As expected the temperature on the trailing edge is slightly higher than in the leading edge. The temperature rises steeply until the end of the plunge. Thereafter, the temperature gradient decreases significantly during the dwell period. Temperatures on both the leading and trailing edges stabilize at around the 50 sec mark which is approximately 34 secs into the dwell period. This is possibly due to a thermomechanical stability attained by the process. It can be clearly observed that at the end of the plunge stage, the temperatures reached approximately 200 °C at both the trailing and leading edges, with possibly higher temperatures beneath the tool pin. This suggests that, at the end of the plunge, it is very likely that the material had softened significantly due to high temperatures, which resulted in a lower axial load. From the axial load and temperature variations, it is clear that a steady state condition is not possible in case of the plunge phase, which corroborates the suggestion by Santella et al [5]. However, if a sufficiently long dwell period is allowed, it was observed that the axial load stabilized almost immediately subsequent to the plunge phase whereas the temperature continued to increase for a significantly long period following the end of plunge.

4.4 *Comparison of ABAQUS simulation with present experiments*

The next step in the research was to compare the results obtained from ABAQUS simulations with the experiments discussed in the previous section. However, there were two primary challenges in this comparison. First, the machine can only be operated manually which made it difficult to plunge with a high plunge speed. For this reason, the plunge speed in the simulation had to be slowed down to reasonably match the plunge

speed of the experiment. In doing so, not only did the computation time increase tremendously, but it also resulted in an unstable simulation towards the end of the plunge stage. The second challenge, unlike the simulation, was to maintain a uniform plunge speed during the experiment. Obviously, this impacts the thermomechanical process. Despite these two challenges, the simulations were compared for the initial 5 secs of the plunge.

A model was generated with the workpiece and tool dimensions similar to the ones used in the experiments. The model and tool dimensions are shown in Fig. 4-5 and Fig. 4-6 respectively. The model was meshed with 1024 C3D8RT elements. Also, the tool pin was modified to have a rounded bottom surface similar to the stir tool used during the experiments. The plunge velocity was slowed down to 0.45 mm/sec to reasonably match the approximate experimental velocity. The tool was plunged for a period of 5 secs into the AA 2024 workpiece. The boundary conditions for this model were kept the same as the earlier ones. A comparison of temperature and axial force are shown in Fig. 4-7 and Fig. 4-8. From the comparison of the temperatures, it can be seen that, the experimental results correlate well with the simulations. From the figure, it can be clearly seen that around the 5 sec mark, the rise in the simulation temperatures is not as rapid as that of the experiment. Similarly, the calculated and measured axial force on the tool matched closely until the 4.5 sec mark. Beyond that, the axial force of the experimental data experienced a sharper increase, as compared to the simulation data. Since, in the case of the experiment the plunge velocity was non-uniform, it is possible that the plunge depth at 5 *secs* was higher than the corresponding depth at 5 secs in the

case of the simulation. A higher plunge depth would mean a higher temperature and axial force.

4.5 *Summary*

In the second stage of the research on the plunge phase, experiments were conducted by plunging into coupons of aluminum alloy 2024-T3 and the temperatures and axial load were measured. The results from these experiments were different from the first FEA simulation and experiments conducted by Gerlich et al due to the fact that these experiments were conducted using a manually controlled milling machine resulting in significantly slower plunge rates. Also, a second FEA model was created to compare with the present set of experiments. A good correlation was observed for the first 5 secs of the plunge after which the simulation experienced convergence problems.

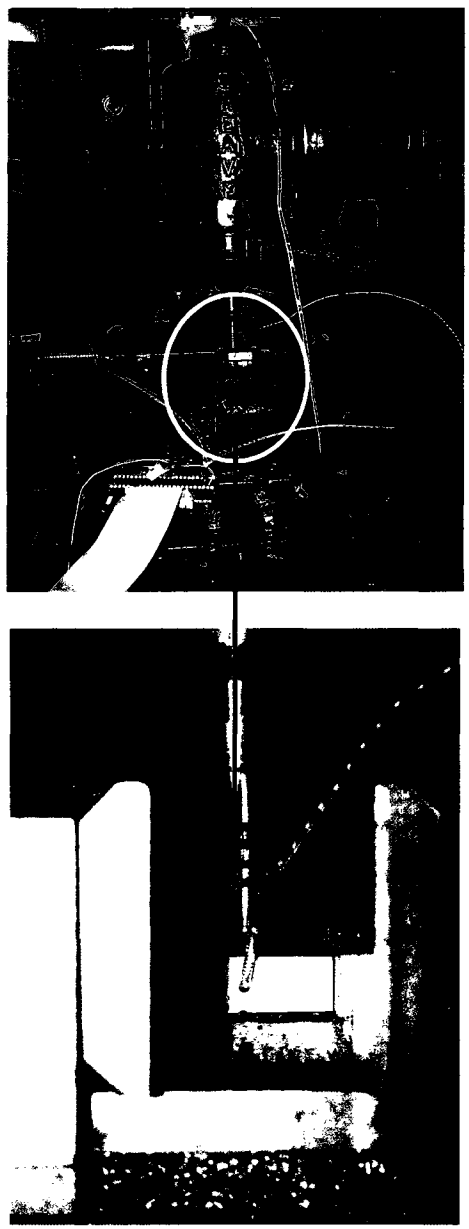

Fig. 4-1 Experimental setup for FSW plunge testing on aluminum 2024 [1]

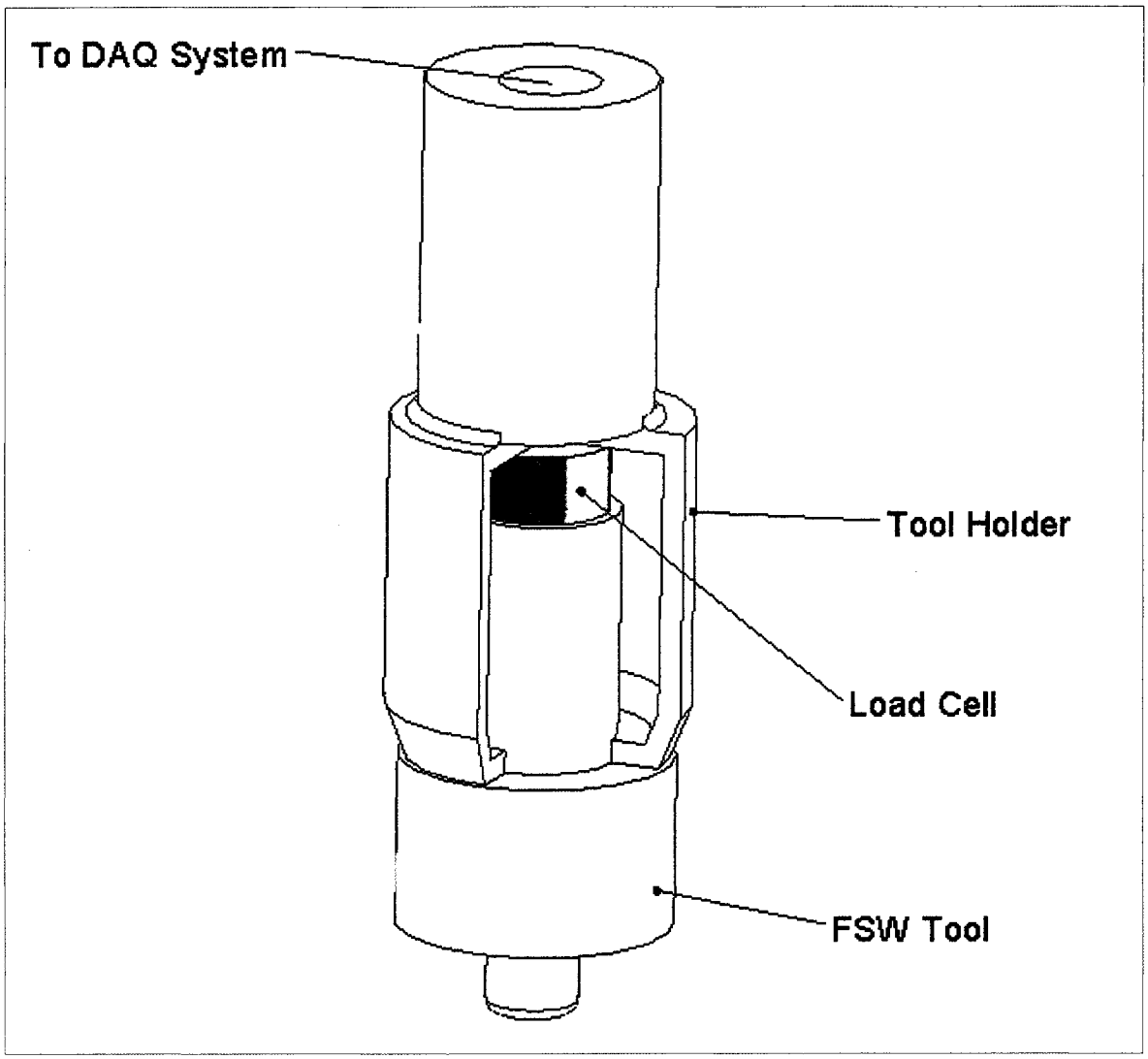

Fig. 4-2 Schematic of load measurement technique during experiments [1]

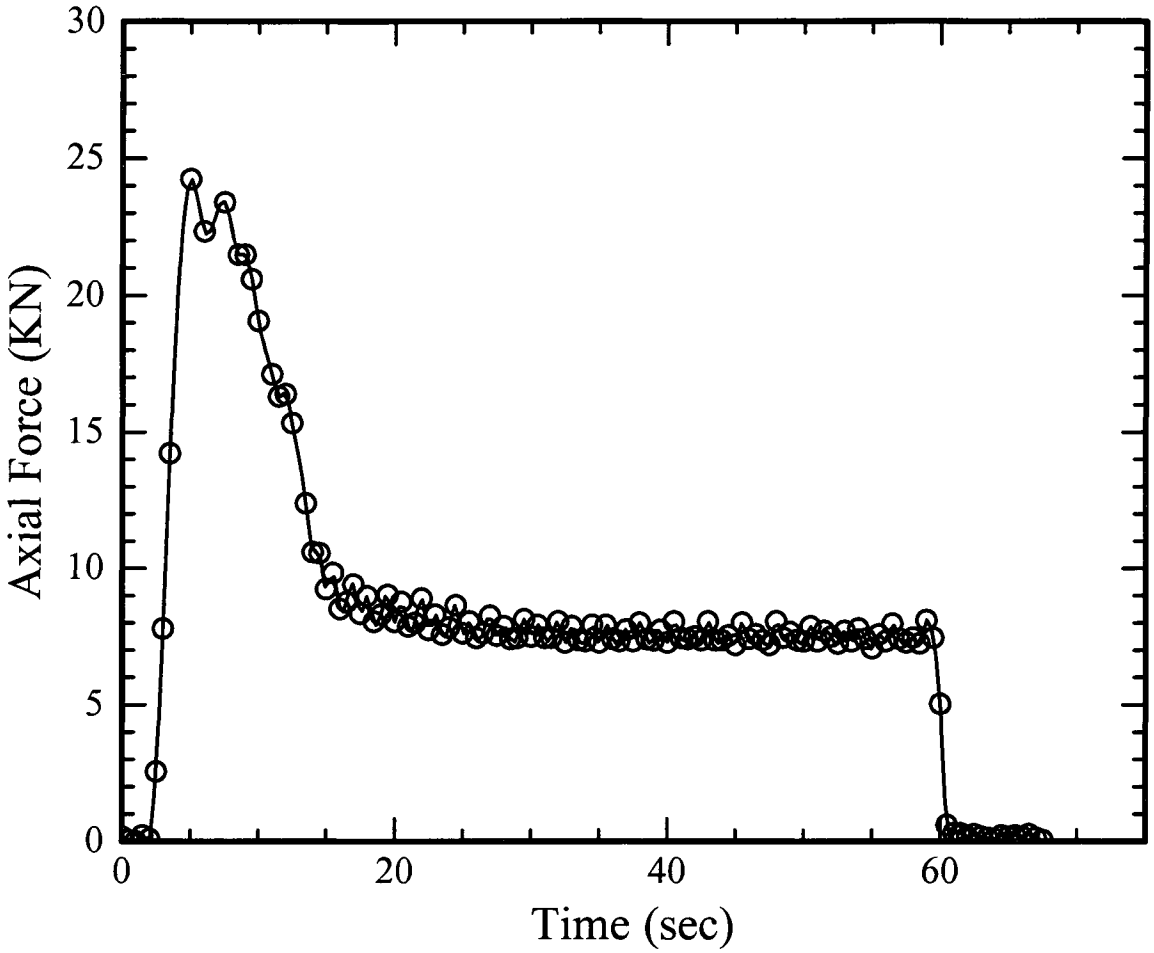

Fig. 4-3 Axial load data from plunge experiment [1]

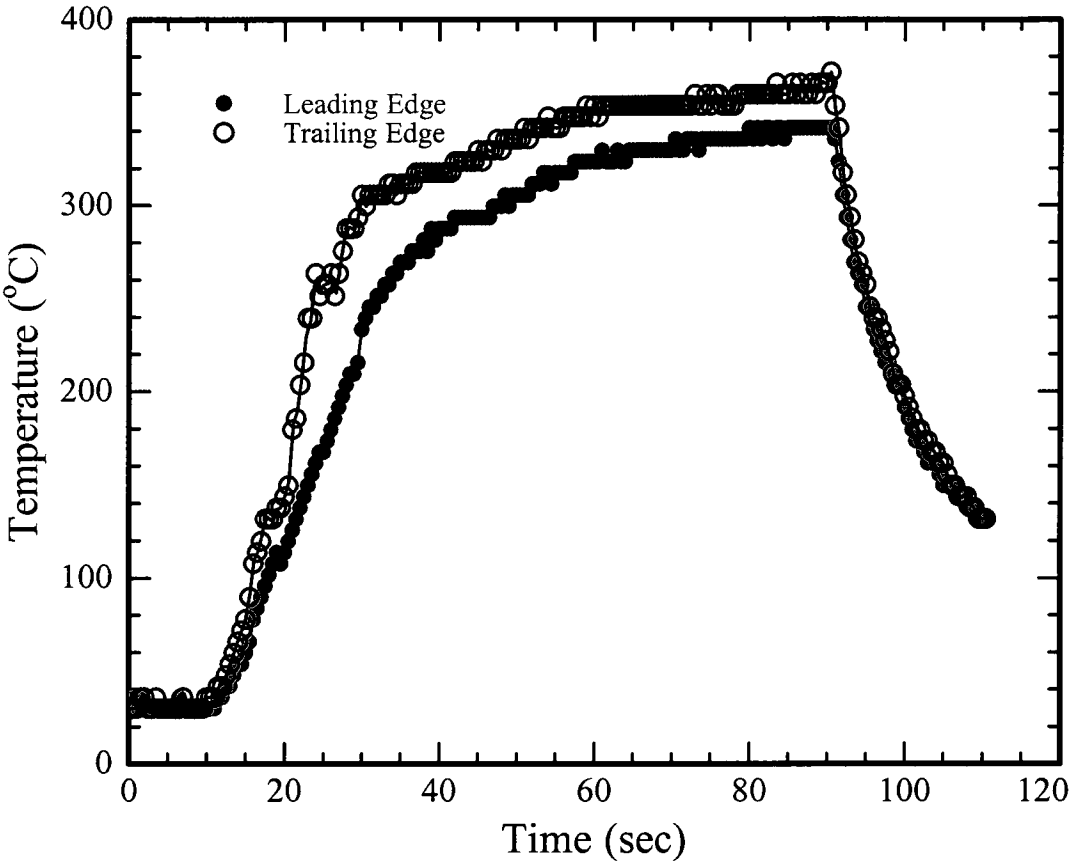

Fig. 4-4 Temperature data from plunge experiment [1]

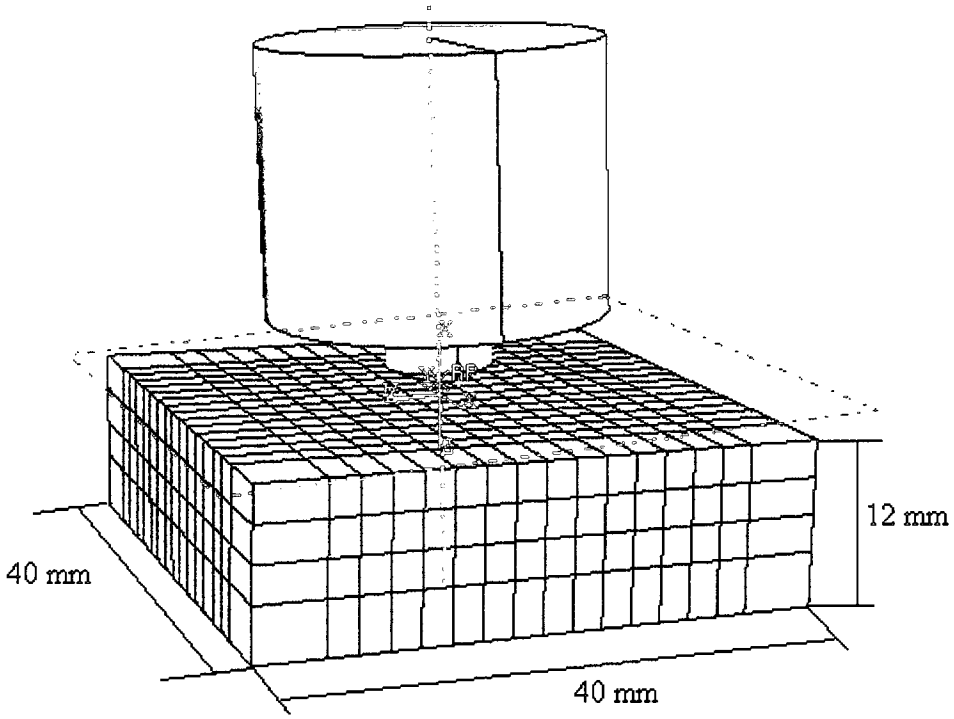

Fig. 4-5 Numerical model for comparison with experiments [1]

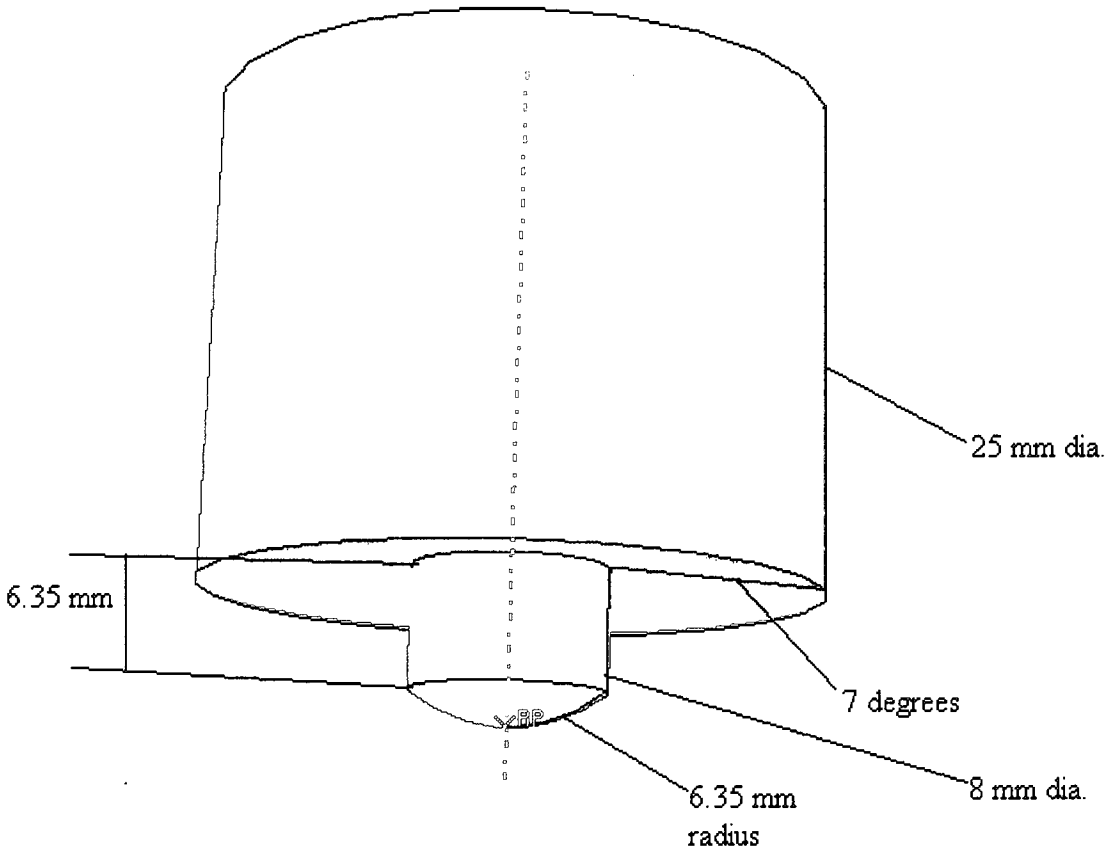

Fig. 4-6 Tool design for comparison between present experiment and simulation [1]

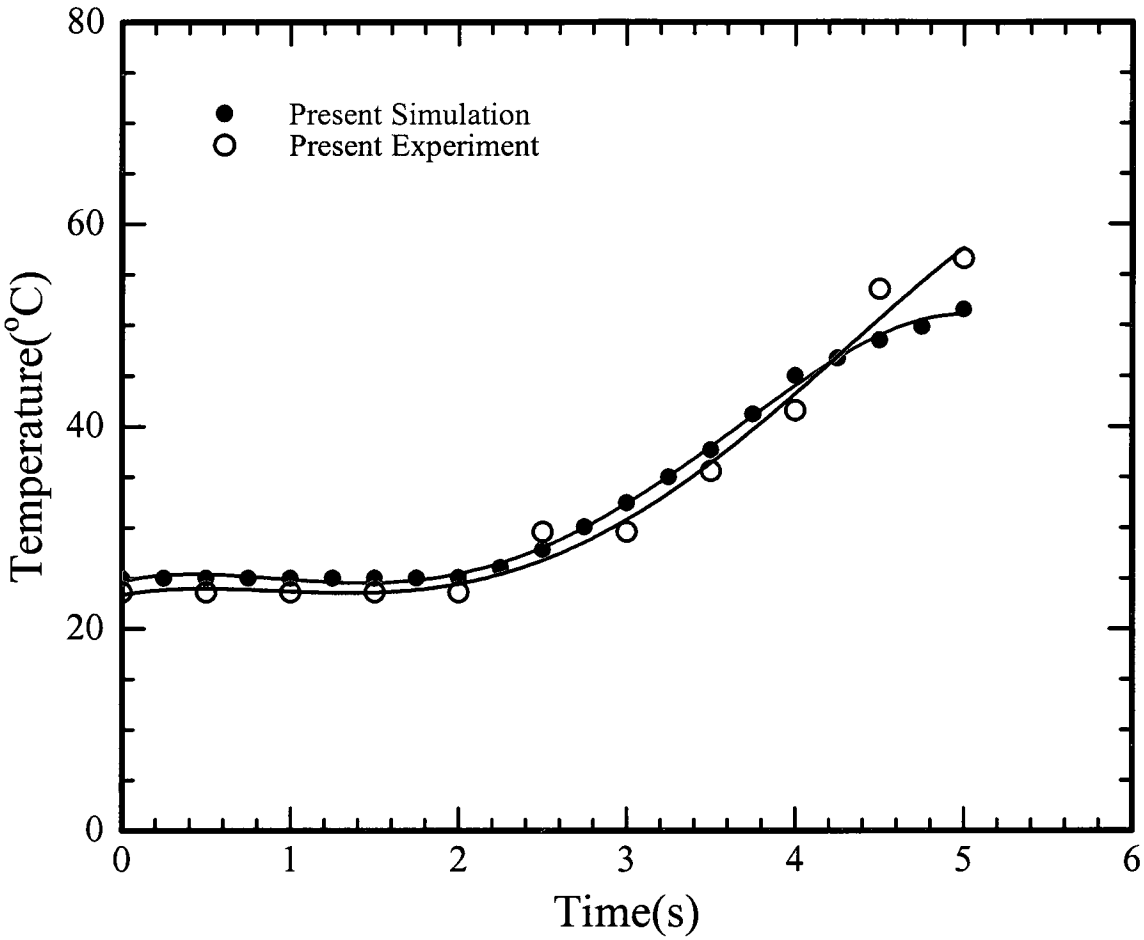

Fig. 4-7 Temperature comparison between present experiment and simulation [1]

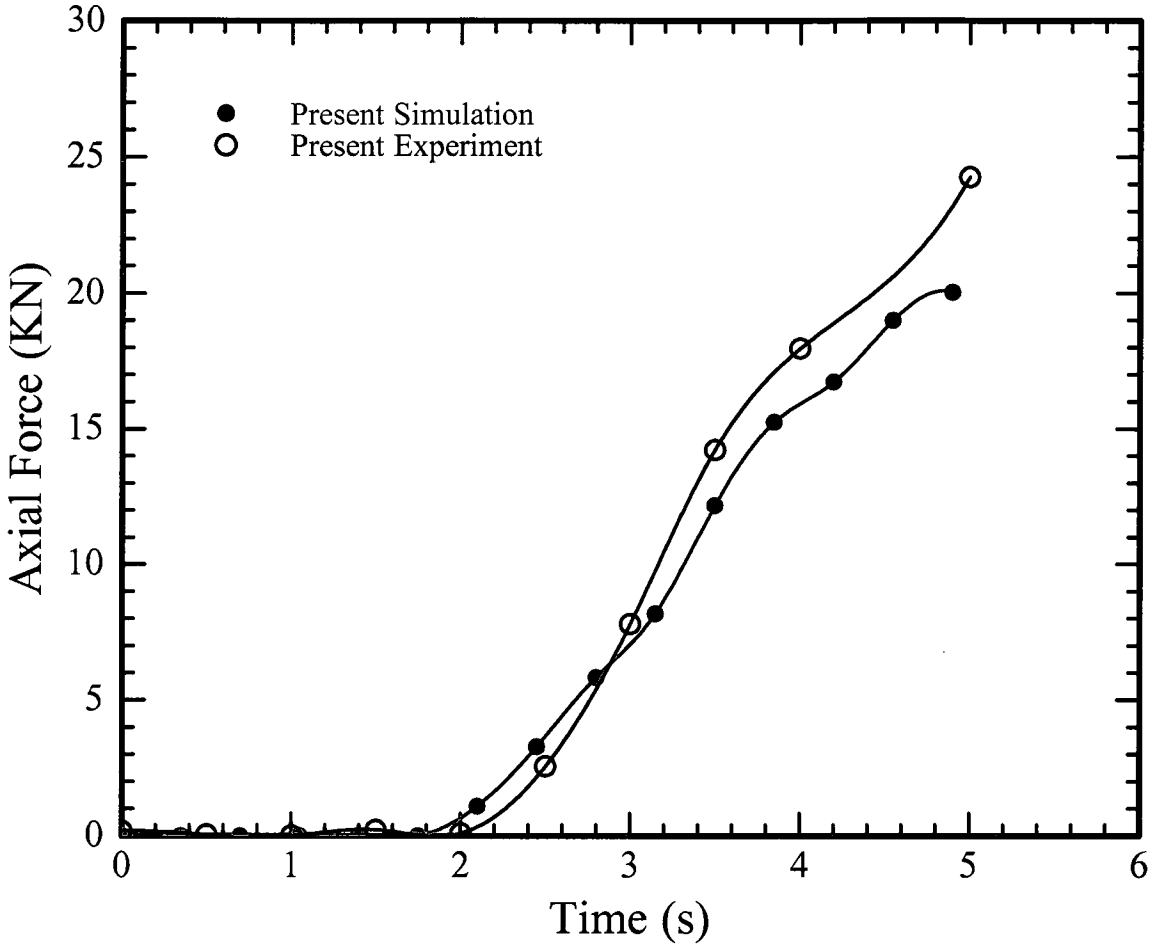

Fig. 4-8 Axial load comparison between present experiment and simulation [1]

References

1. Mandal, S., Rice, J., Elmustafa, A.A., 2008, "Experimental and numerical investigation of the plunge stage in friction stir welding" *Journal of Materials Processing Technology*, pp. 411-419.

2. Mitchell, J.E., Cook, G.E., Strauss, A. M., "Force sensing in friction stir welding" *6th International Trends in Welding Research Conference Proceedings,* Pine Mountain, Georgia, April 15 –19, 2002.

3. Henderson, L.T., "Initial load characteristics for an aluminum alloy friction stir weld" M.S. Thesis, Old Dominion University, 2006.

4. Gerlich, A., Su, P., Bendzsak, G.J., North, T.H., 2005, "Tool penetration during friction stir spot welding of Al and Mg alloys" *Journal of Materials Science*, pp. 6473–6481.

5. Santella, M., "Plunge testing to evaluate tool materials for friction stir welding of 6061+20wt% Al_2O_3 composite" *4th International Friction Stir Symposium,* Park City, Utah, May 14-16, 2003.

Chapter 5

Numerical Analysis of Donor Material Concept

Tool wear is a significant hindrance in producing long, continuous welds in harder materials such as steel. One of the requirements to successfully incorporate FSW for manufacturing large units that are typical of shipbuilding and railways industries is the production of long continuous welds. The demand for joining harder materials with FSW justifies research on tool wear and its mitigation. It is well documented that a large fraction of the tool wear occurs during the initial plunge phase of the weld [1-5]. The donor material approach is a novel concept in reducing tool wear at the plunge region [6].

5.1 *Concept of Donor Material*

The basic idea behind this concept is to provide localized pre-heating at the plunge area using a softer material as a donor. A two-dimensional schematic is shown in Fig. 5-1. As the tool penetrates through the softer donor material, it generates heat due to friction between the tool pin and the donor material and also due to plastic work in the material. The heat generated is transferred into the harder workpiece material beneath the donor by conduction. This pre-heats the workpiece at the plunge area resulting in material softening. A softer workpiece material would result in lower flow stresses, thus reducing tool wear. One of the challenges of the donor material concept is the positioning of the donor material on top of the workpiece material. It is critical that the placement of the donor is relatively simple to reduce production time and cost. Fig. 5-2 shows a three-dimensional representation of the positioning of the donor material. It is feasible to

machine a slot in the joint line in the region where the weld is to be initiated. The soft donor material is placed into the slot and the tool is plunged onto it. For this concept to be successful, it is crucial for the donor material to have a sufficiently high thermal conductivity to allow heat transfer into the workpiece at a rapid rate. This is necessary so that by the time the tool pin approaches the workpiece, the latter is warm enough to permit an easier penetration.

5.2 *Wear Models*

A basic discussion on the various material wear models is useful to gain a better perspective of the mechanism of the donor material approach for FSW. Xie et al [7] developed a two-dimensional model to estimate tool wear in turning operations in terms of process variables such as contact pressure at tool/chip and tool/work interface, relative sliding velocity and cutting temperature distribution at steady state. Usui et al [8] developed a wear rate model for machining processes, which quantifies wear based on the cutting process variables and is given by the equation,

$$\dot{w}=C\nu_s\sigma_f \exp\left(\frac{-\lambda}{\theta_f}\right) \tag{5.1}$$

where $\dot{w}$ is wear rate, i.e., the wear volume per unit area and unit time; ν_s is the relative sliding velocity at tool/work interface; σ_f is the contact pressure; θ_f is the absolute temperature, C and λ are constants determined for the combination of a tool and a work material. Assuming that the relative sliding velocity is the same for the entire plunge process, it is evident that the wear rate is directly proportional to the contact pressure. A

very popular wear model is the Archard's equation or one of its modifications as proposed by Felder et al [9] which incorporates microstructural and chemical properties of the tool and the workpiece and is given by,

$$w = \int K_f K_w \frac{\sigma_f \cdot v_s}{H_v^m (microstructure(\Theta_s), \Theta_s)} f\left(\frac{H_v}{H_{va}}\right) \cdot dt \tag{5.2}$$

where w is the wear; K_w is a constant that depends on the chemical composition of the tool; K_f is a constant that depends on the tool workpiece interface; v_s is the relative sliding velocity at tool/work interface; σ_f is the contact pressure; H_v is the microhardness; H_{va} is the microhardness of oxides present and Θ_s is the temperature on the tool surface. Tercelj et al [10] characterized the above equation as very useful for nitride tools. Vardan et al [11] proposed a simple wear equation based on the relative sliding velocity, temperature on the tool surface and contact pressure.

$$w = \frac{\left(v_s^{\alpha} \cdot \theta_s^{\beta} \cdot \sigma_f^{\lambda}\right)}{10000} \tag{5.3}$$

where w is the wear; α, β, λ are exponents obtained by a regression analysis; v_s is the relative sliding velocity at tool/work interface; σ_f is the contact pressure; θ_s is the temperature on the tool surface. Based on all the above wear models, it is very clear that a very direct relation exists between contact pressure and tool wear. So, if it was possible to reduce contact pressure at the tool workpiece interface, it is very likely that the wear rate also could be reduced.

Gerlich et al [12] studied the wear during friction stir spot welding in aluminum and magnesium alloys. They based their investigation on the wear maps developed by Zhang et al [13]. Based on these wear maps, they characterized wear in FSW into three types – mild, severe and melt wear. The wear map is shown in Fig. 5-3. The ordinate in this diagram is the normalized force, $\overline{F} = F/A_n H_0$ where F is axial load, A_n is the nominal area of contact at the sliding surface and H_0 is the hardness of the material at room temperature. The abscissa is the normalized velocity, $\overline{v} = v r_0/a_{eff}$ where v is the sliding velocity, r_0 is the length of the contact area and a_{eff} is the mean thermal diffusivity of the tool and the workpiece. According to Zhang et al [13], mild wear is typically characterized by plastic shearing and nucleation and propagation of sub-surface cracks which create wear debris when they reach the surface. Gerlich et al [12] demonstrated that mild wear can start as early as when the tool pressure reaches 1 MPa. In the current research, a tool pin diameter of 10 mm is used. With a pin diameter of 10 mm the cross-sectional area at the base of the pin is 78.5 mm^2. This means that to reach a pressure of 1 MPa, the axial load has to exceed 78.5 N. This occurs almost immediately as the tool contacts the workpiece. Thus, mild wear starts immediately upon starting the plunge. As the plunge proceeds, a transition from mild to severe wear occurs. According to Zhang et al [13], this transition occurs as low as 10 MPa. Therefore, in the current case, severe wear would start at a load of only 785 N. A characteristic of severe wear is that thermally activated deformation processes promote softening of the material immediately adjacent to the contact interface [13], and therefore, the base of the rotating pin becomes coated

with an adhering layer of the workpiece material. Based on the forces and the sliding velocity Gerlich et al [12] demonstrated that the process enters a melt wear phase shortly after the plunge starts and once this phase initiates, this continues to be the dominant wear mechanism. They also point out that the standard wear maps typically include the effects of oxidation wear. However, in the case of a friction stir welding plunge, the exposure to oxidation is negligible. Hence, oxidation wear can be excluded in this case. In a standard case of sliding, melt wear transitions to oxidation wear.

Based on the above discussion, it is evident that wear rate is directly proportional to the axial force, contact stress and contact pressure. Therefore, a reduction of the axial force and contact stresses should reduce tool wear. This dissertation uses FEA to evaluate the donor material concept and its effectiveness to reduce the forces and contact stresses during the plunge phase of FSW.

5.3 *Numerical Model*

The numerical modeling of FSW poses a challenge due to high strain rates and temperatures involved in the process resulting in a complicated, problem involving non-linear material behavior. Simulation of the entire process was performed using an elasto-plastic constitutive law available in ABAQUS finite element code. ABAQUS is used due to its strong capabilities of handling non-linear problems and the built-in Johnson-Cook material law which is used in the present problem. The model consists of a deformable workpiece and a rigid stir welding tool. The tool was plunged into a 100 mm x 100 mm x 20 mm workpiece for a period of 3 sec upto a distance of 11 mm. A central square piece

of donor material measuring 60 mm x 60 mm is placed on top of the workpiece material. The depth of this central piece was adjusted to simulate different thicknesses of the donor material. The ABAQUS partition tool was used to partition the model into donor and workpiece and allowed for defining different materials for the workpiece and donor. This was done to simplify the simulation as the use of two separate deformable bodies, for the donor and workpiece would mean that a contact condition would have to be defined between them, which would make the simulation more complicated and also require tremendous amounts of computation time.

A pure Lagrangian approach was adopted for the simulation and this resulted in solution convergence without premature termination due to excessive element distortion. The workpiece is meshed using 8 node coupled temperature displacement, brick elements (C3D8RT). Using these initial parameters in the FEA model, different mesh densities were investigated. Normally, a higher mesh density provides for higher accuracy but also increases the computational time; therefore, a trade-off between time and accuracy becomes crucial. The mesh was graded in a way that provides for a higher mesh density around the tool plunge area. This improves the accuracy of the solution around the tool without tremendously increasing the computational time. The graded meshes are obtained by partitioning the workpiece into smaller cells. The workpiece was initially meshed with 1600 elements with a higher mesh density closer to the tool with a similar distribution maintained right along the thickness. In the subsequent models, a higher mesh density was used on the donor material close to the penetration area increasing the number of

elements to 2000. Mesh densities of 3388 and 4608 elements were also attempted. However, a convergent solution could not be obtained in a reasonable amount of time.

The finite element mesh is shown in Fig.5-4. The tool dimensions used in the model are shown in Fig.5-5. The workpiece is constrained at the bottom surface to prevent the bending of the surface and the sides are constrained such that there is no deformation along the boundary other than compression along the tool plunge direction. The tool is modeled as a rigid surface with no thermal degrees of freedom. For the contact conditions between the tool and the workpiece, the tool is modeled as a master surface and the workpiece as a slave. A constant friction coefficient of 0.3 is assumed between the tool and the workpiece [14] and the penalty contact method is used to model the contact interaction between the two surfaces. The tool rotational speed is set at 300 RPM and the tool plunge velocity is set to a uniform value of 4 mm/s.

5.4 *Results and Discussion*

Two different depths of donor material were analyzed to investigate the effects of depth of the donor on axial force and contact stresses during a plunge. In the first case the donor material was set at 50% of plunge depth, and in the second case the donor material was set to 75% of plunge depth. This means that in the first case, the tool would travel 50% of its total plunge distance through a softer donor material and the remaining 50% through steel. Similarly, in the second case, the plunge through the donor is 75% of the plunge distance and the remaining 25% of the plunge is through steel. For this entire study, the workpiece material was fixed to AISI 1045 steel, a common low carbon steel.

One of the critical factors in this novel approach is the selection of the appropriate material for use as donor. This would obviously vary depending on the workpiece on which the actual weld is to be made and will require a significant amount of experimentation before the right donor material is selected, which can be a subject of research in its own right. In this research, the candidate materials selected as donor are copper and the aluminum alloys AA 2024 and AA 6061. The alloy compositions of the donor materials, AA 6061 and AA 2024 are shown in Table 5.1 and Table 5.2 and the composition of the workpiece, AISI 1045 steel is shown in Table 5.3. Aluminum alloys are relatively soft materials as compared to steel and provide good thermal conductivity for conduction of heat from the donor to the workpiece. Two other factors which make the selection of aluminum alloys appropriate for this particular research is that there is a significant amount of research done on aluminum alloys in the case of FSW, and also a significant amount of research was done on simulating plunges into aluminum alloys during the course of this dissertation, thus making it easier to extend the plunge simulation to that of donor material simulations. The high thermal conductivity and low hardness values of copper make it a very attractive candidate as a donor material, but despite being a relatively soft material, its density is very similar to steels and the melting point is two-thirds that of steel and much higher than that of aluminum. The temperature and strain rate dependent elastic-plastic Johnson-Cook law was again selected for this set of simulations. The Johnson-Cook constitutive law is given by the equation,

$$\bar{\sigma} = \left[A + B\left(\bar{\varepsilon}^{pl}\right)^{n}\right]\left[1 + C\ln\left(\frac{\dot{\bar{\varepsilon}}^{pl}}{\dot{\varepsilon}_0}\right)\right]\left(1 - \hat{\theta}^{m}\right) \tag{5.4}$$

This constitutive law is discussed in detail in chapter 4. The Johnson-Cook parameters for all the three candidate donor materials and the AISI 1045 steel workpiece are given in Table 5-4. Other thermal and mechanical properties used in this model are listed in Table 5-5. As shown in Fig. 5-4, a square sample of 60 mm x 60 mm in the center of the workpiece material is defined as the donor material. In the first case, the depth of the donor is set at 5 mm and in the second case the depth is set to 7.5mm. All the elements in the central square were defined as either, AA 2024, AA 6061 or copper for the different cases being simulated.

In Fig. 5-6 the axial force on the tool is plotted versus time, in case of a plunge into a regular 1045 steel and into a combination of donor material and the steel. The donor material extends to 50 percent of the depth of plunge or 5 mm. The three donors AA 2024, AA 6061 and copper are represented in the plot. From the figure, it is clearly evident that the use of a donor material significantly decreases the axial force on the tool. In case of the plunge into a regular AISI 1045 steel workpiece the axial load reaches upto 78 kN while in the case of a combination of 50 percent AA 2024 and steel the peak load is only 17 kN. Similarly, in the case of a donor of 6061 and copper the peak loads are 16 kN and 20 kN respectively, which is roughly one fourth of the peak load of plunging directly into steel. Fig. 5-7 compares the axial loads with similar materials but with a donor material thickness of 75 percent of the plunge depth or 7.5 mm. Even in this case, the forces are much lower than those of the regular steel. In the case of a combination of 75 percent AA 2024 and steel the peak load is only 13 kN. Similarly in the case of a donor of AA 6061 and copper the peak loads are 14 kN and 11 kN respectively. Based on

the earlier discussion on the wear map developed by Zhang et al [13] shown in Fig. 5-3, it is evident that with the decrease in axial force, wear decreases, assuming that the sliding velocity stays the same. As the rotational velocity of the tool is assumed constant, the sliding velocity is constant as well. Fig. 5-8 compares the contact stress at the tool workpiece interface with and without the donor in case of a plunge with 50% donor and Fig. 5-9 is a similar comparison with 75% donor. In the case of a direct plunge into AISI 1045 steel without the use of a donor material the peak stress is close to 30 kPa. In comparison, the peak stress in steel in combination with 50% AA 2024, donor material is 8 kPa. The stresses are even lower when copper and AA 6061 are used as donors. A similar effect is also observed when using a combination of steel with 75% donor. From these simulations, it is evident that if a plunge into regular steel is modified to include a softer donor material whose thickness is 50% or 75% of the plunge depth, a substantial reduction in contact stresses and axial load can be attained. This should be beneficial in mitigating tool wear. Fig. 5-10 compares the external work into the system for a plunge into 1045 steel alone and 1045 steel with a donor material placed above it. It is clearly evident that the combination of donor material and 1045 steel requires significantly less external work to be input into the system in order to complete a plunge. In order to gain a better perspective on the mechanism of the donor material, temperatures on a node on the surface of the AISI 1045 workpiece were plotted versus time for the various donor materials used, as shown in Fig. 5-11. The graph is plotted for the case of plunge into a combination of 50% donor and steel. Since the tool plunges at uniform speed, it starts to penetrate through the steel at 1.5 sec. At this time, the temperature on steel in the region of the plunge is approximately 130 ^{0}C in the case of a plunge with a AA 2024 donor and

approximately 90 ^{0}C in case of both AA 6061 and copper. This means that the steel has been pre-heated to the above temperatures at the beginning of plunge which obviously translates to lower axial loads and contact stresses that were discussed earlier.

5.5 *Summary*

This chapter proposes a novel concept for providing localized pre-heating of the workpiece material in the region of plunge. A numerical investigation was performed on the effect of positioning a softer donor material on top of a regular 1045 steel workpiece. The heat generated from the plunge into the donor material is thermally conducted onto the workpiece material (steel), thus softening it. Three different donor materials, AA 2024, AA 6061 and copper were discussed. The donor materials were positioned so that they formed 50% and 75% of the plunge depth. It was observed that using a donor material decreased the axial load during plunge by approximately 80%. Additionally, the contact stresses at the tool workpiece interface also decreased by approximately 75% when a donor material was used in the plunge area. The decrease of both axial force and contact stress should contribute to decreasing tool wear. Although the donor material approach does not affect tool wear during the actual weld phase, it can significantly increase tool life by reducing wear in the plunge phase.

Al	Mg	Si	Fe	Other
97%	1.2%	0.8%	0.7%	Trace

Table 5.1 Alloy composition of AA 6061

Al	Cu	Mg	Mn	Other
94.7%	3.8%	1.2%	0.3%	Trace

Table 5.2 Alloy composition of AA 2024-T3

Fe	C	Mn	Other
98.6%	0.45%	0.9%	Trace

Table 5.3 Alloy composition of AISI 1045

	AISI 1045 [17]	AA 2024-T3 [14]	AA 6061-T6 [16]	Copper [15]
A (MPa)	553.1	369	289.9	90
B (MPa)	600.8	684	203.4	292
C	0.013	0.0083	0.011	0.025
n	0.234	0.73	0.35	0.31
m	1	1.7	1.34	1.09

Table 5.4 Johnson-Cook parameters for the workpiece and various donor materials used in the simulation

	AISI 1045 [19]	AA 2024-T3 [18]	AA 6061-T6 [18]	Copper [18]
Thermal Conductivity (W/m-K)	49.8	121	167	386
Specific Heat (J/kg-^{o}C)	7850	875	896	383
Elastic Modulus (GPa)	205	73	68.9	124
Poisson's Ratio	0.3	0.34	0.33	0.34
Density (kg/m^{3})	486	2770	2700	8960

Table 5.5 Mechanical and thermal properties used in the model

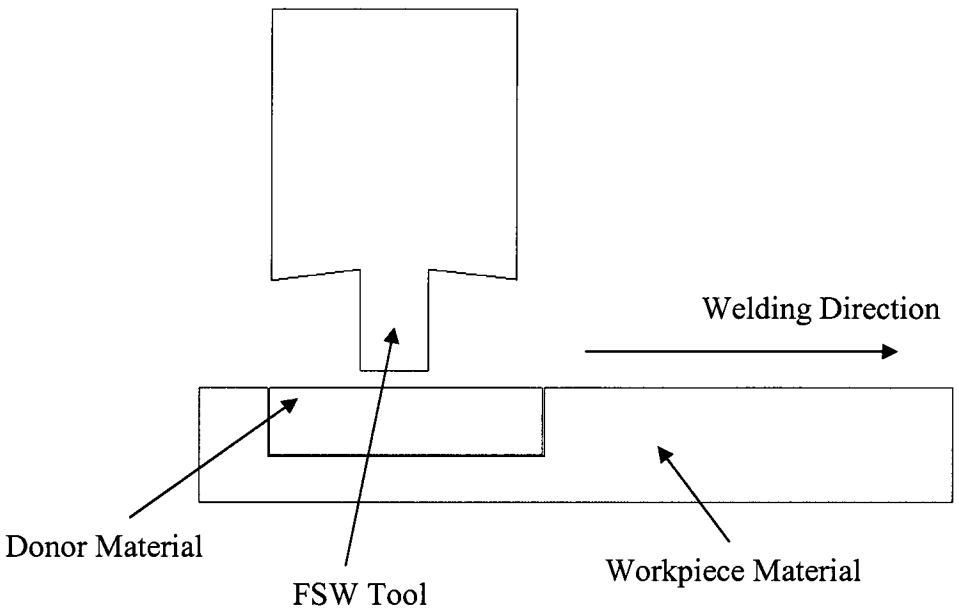

Fig. 5-1a FSW tool plunging through a donor material and preheating the workpiece

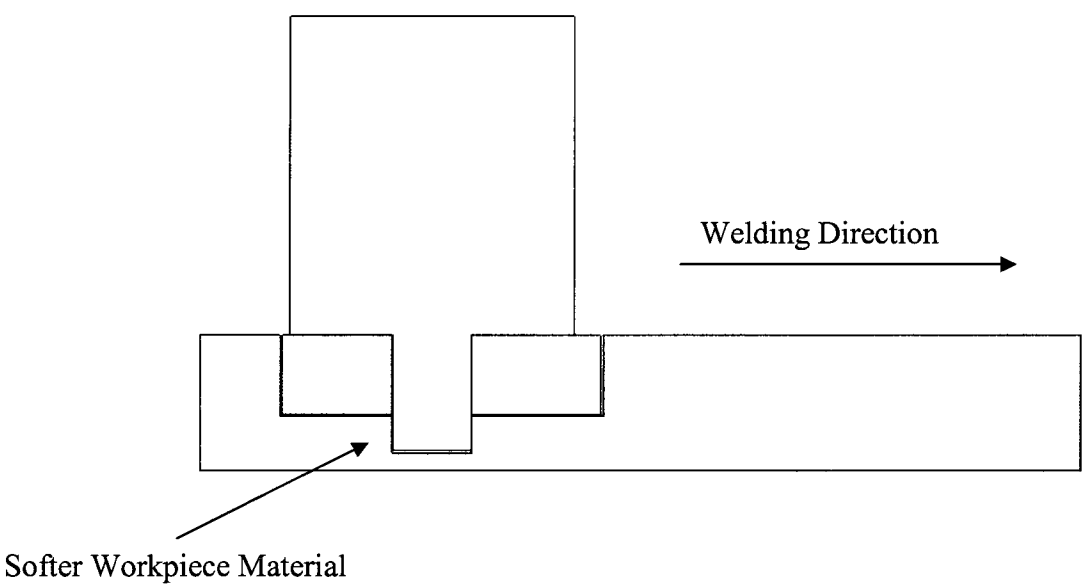

Fig. 5-1b Tool completes a plunge into softer workpiece material

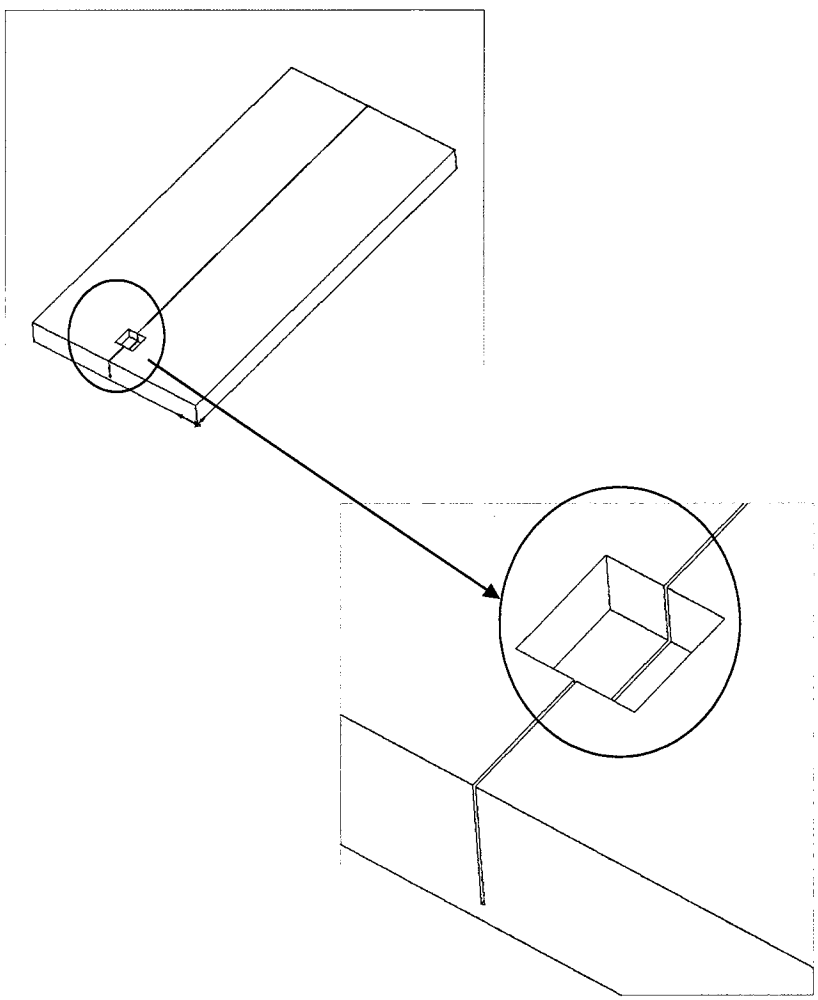

Fig. 5-2 Illustration of slots machined to accommodate a donor material

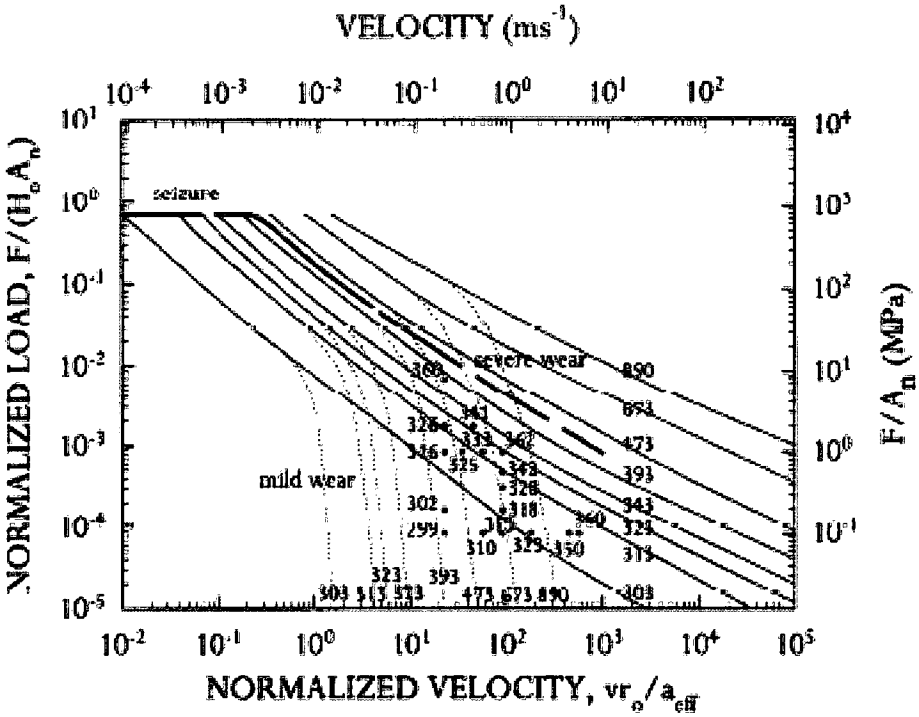

Fig. 5-3 Wear characteristics in SAE 52100 Steel [13]

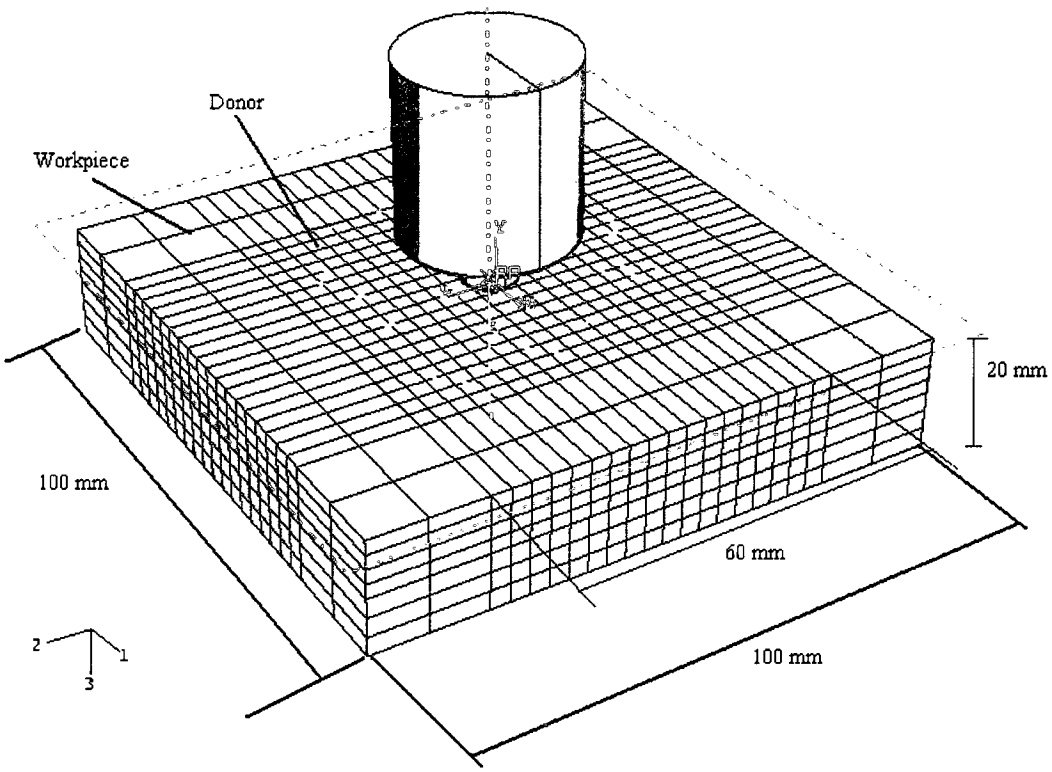

Fig. 5-4 FEA mesh for donor material simulation

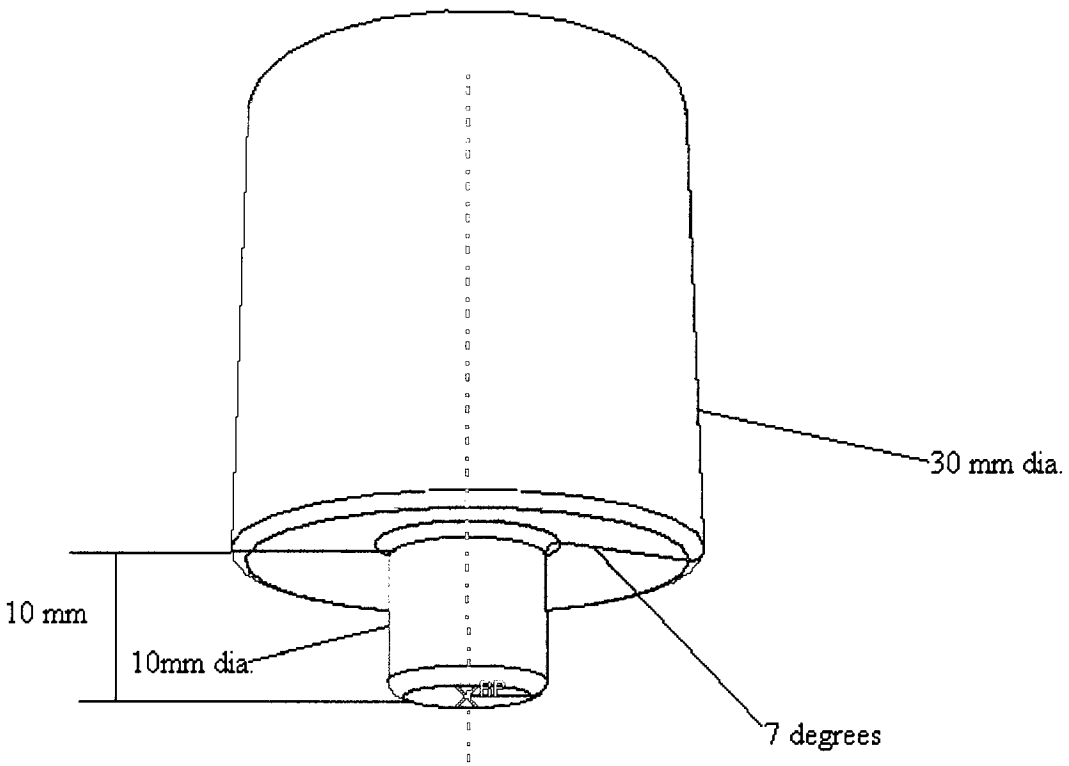

Fig. 5-5 Tool design for simulation

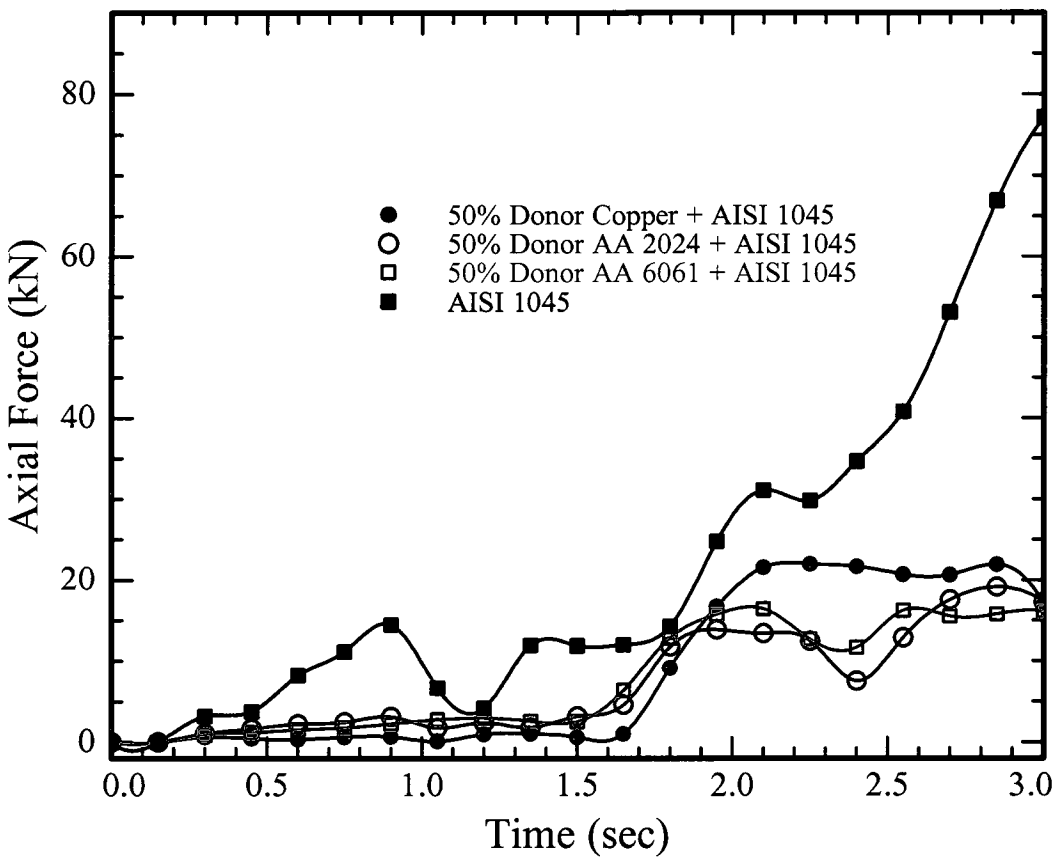

Fig. 5-6 Comparison of axial forces on tool in case of using 50% donor material

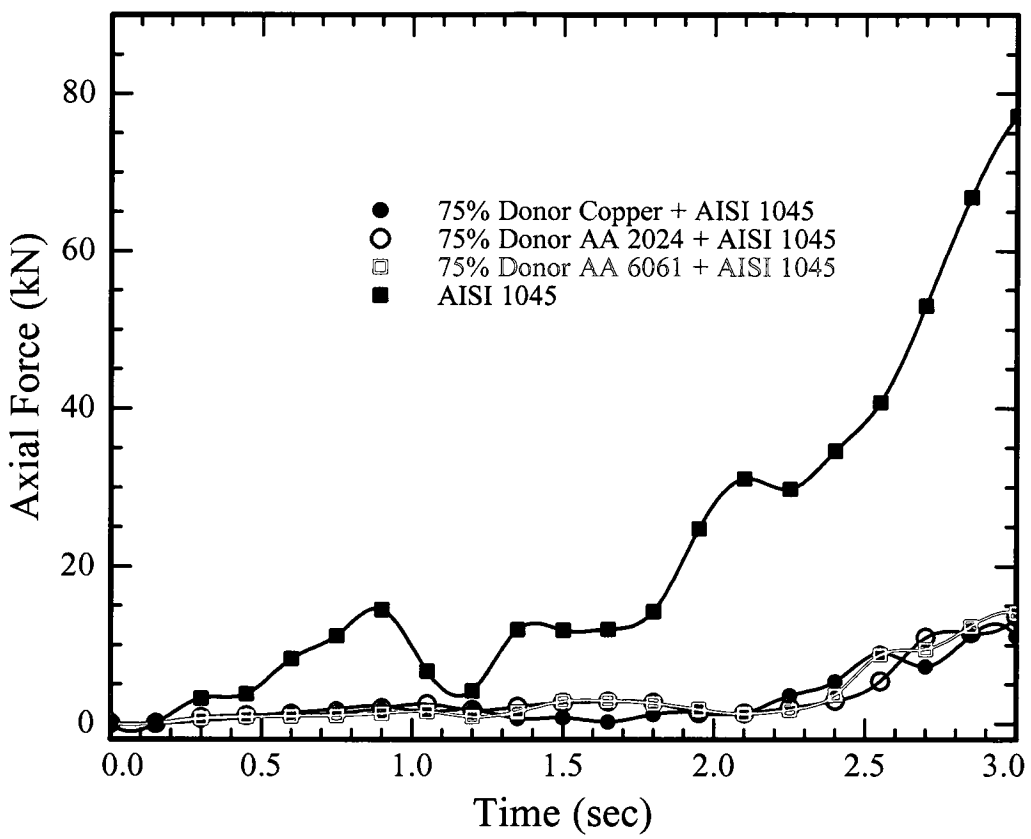

Fig. 5-7 Comparison of axial forces on tool in case of using 75% donor material

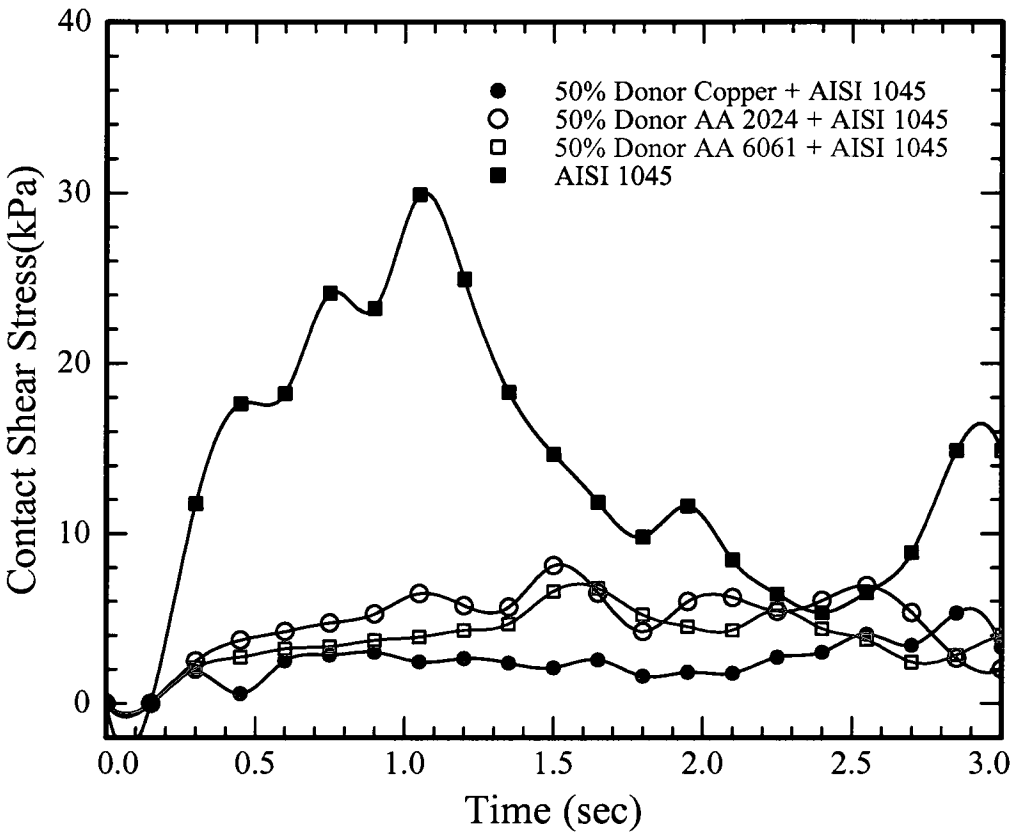

Fig. 5-8 Comparison of contact stress tool/workpiece interface in case of using 50% donor material

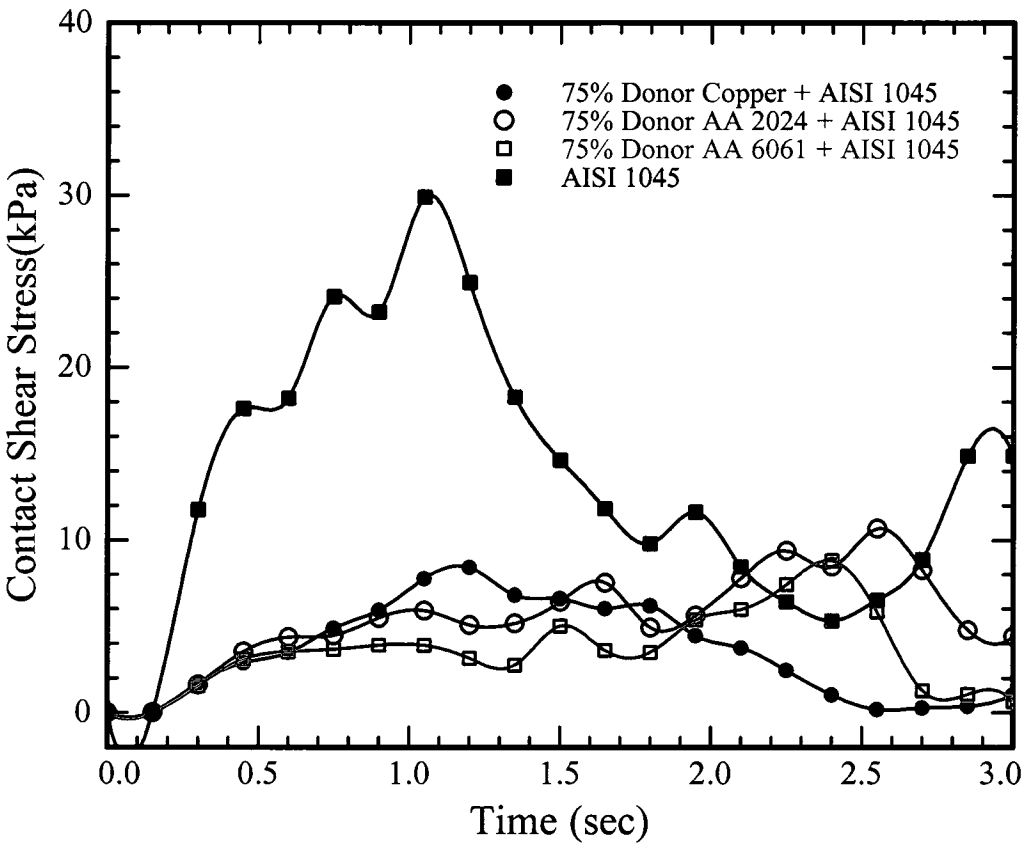

Fig. 5-9 Comparison of contact stress tool/workpiece interface in case of using 75% donor material

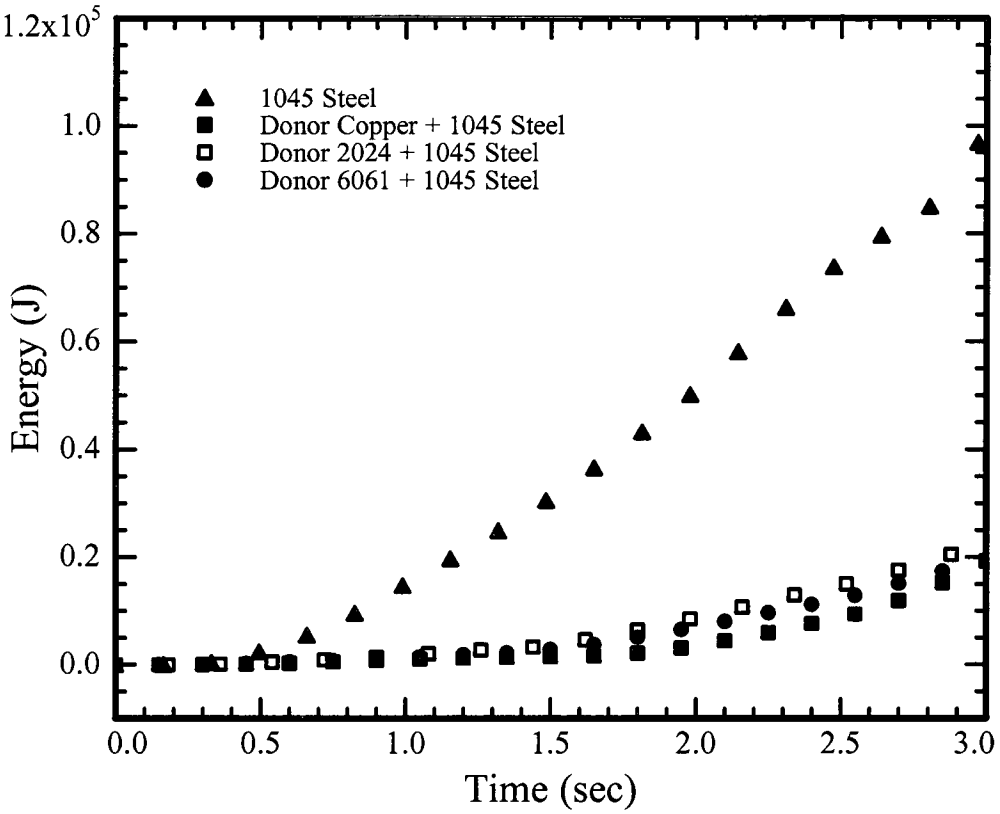

Fig. 5-10 Comparison of total work done in 1045 Steel alone and combination of 50% Donor material and 1045 Steel

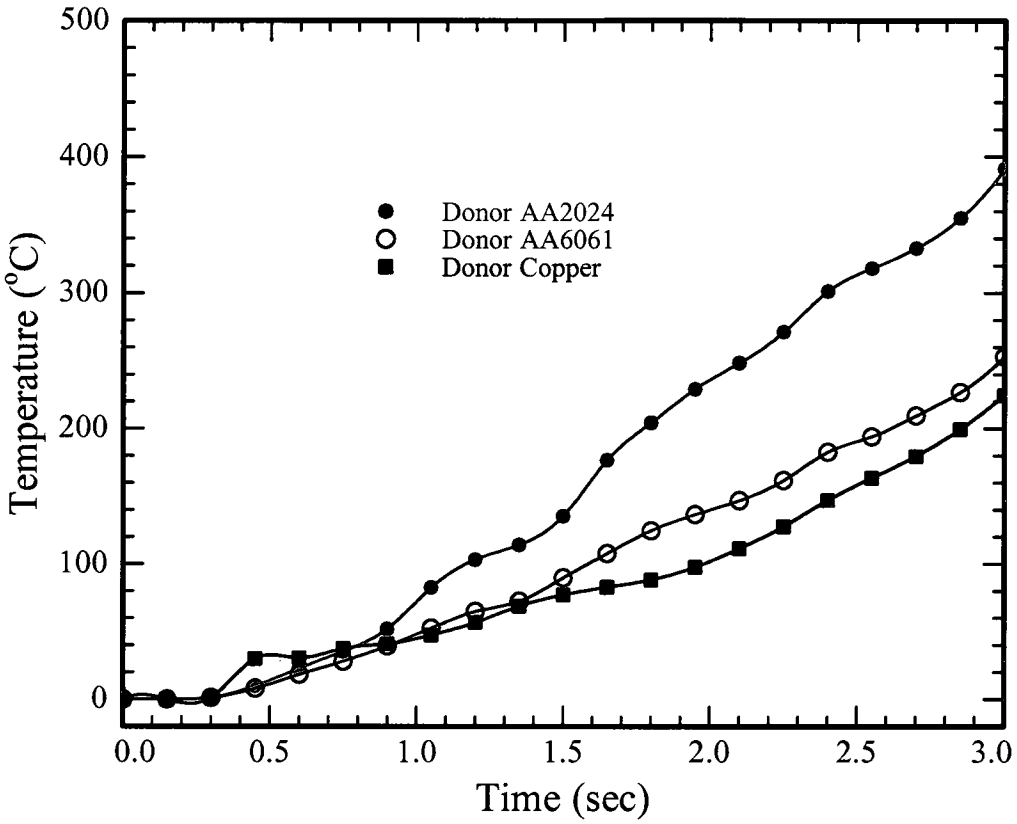

Fig. 5-11 Temperature on top of steel workpiece through the plunge in the case of 50% donor

References

1. Thomas, W., "Friction Stir Welding of Ferrous Materials; A Feasibility Study" *Proceedings of First International Symposium on Friction Stir Welding,* Thousand Oaks, California, June 14-16, 1999.

2. Thomas, W., 1999, "Feasibility of Friction Stir Welding Steel" *Science and Technology of welding and joining,* Vol. 4, pp. 365-372.

3. Lienert T.J., Stellwag W.L. Jr., Grimmett, B.B. and Warke, R.W., 2003 "Friction stir welding studies on mild steel" *Supplement to the Welding Journal*, pp.1s-9s.

4. Mandal, S., Williamson, K., 2006, "A thermomechanical hot channel approach for friction stir welding" *Journal of Materials Processing Technology*, pp.190-194.

5. Mandal, S., "Analytical model of a thermomechanical hot channel coupled to a friction stir welding process" *M.S. Thesis*, Old Dominion University, 2003.

6. Donor material technology for friction stir welding, U.S. Provisional Patent Application No. 61/070,642.

7. Xie, L.-J., Schmidt, J., Schmidt, C., Biesinger, F., 2005, "2D FEM estimate of tool wear in turning operations" *Wear*, pp. 1479-1490.

8. Usui, E., Shirakashi, T., Kitagawa, T., 1978, "Analytical prediction of three dimensional cutting process, part 3: cutting temperature and crater wear of carbide tool, *Transactions of ASME Journal of Engineering Materials Technology*, pp.236–243.

9. Felder, E., Mahjoub, K., "Wear prediction of hot working tool: Physical phenomena and modelisation" *First ESAFORM Conference on Metal Forming*, 1998, pp. 93-96.

10. Tercelj, M., Perus, I., Turk, R., 2003, "Predicting of tool wear for hot metal forging – an overview and suggested new approach" *RMZ-Materials and Geoenvironment*, pp. 589-605.

11. Vardan, O.T., Bagchi, A., Altan, T., "Investigation of die wear in upsetting using FEM code ALPID" *Proceedings of the 15th North American Manufacturing Research Conference*, May 27-29, 1987, pp. 386-393.

12. Gerlich A., Su, P., Bendzsak, G.J., North, T.H., 2005, "Tool penetration during friction stir spot welding of Al and Mg alloys" *Journal of Materials Science*, pp. 6473–6481.

13. Zhang, J., Alpas, A. T., 1997, "Transition between mild and severe wear in aluminium alloys" *Acta Materialia*, pp.513 – 528.

14. Schmidt, H., Hattel, J., Wert, J., 2005, "A local model for the thermomechanical conditions in friction stir welding" *Modeling and Simulation in Materials Science and Engineering*, pp. 77-93.

15. Johnson, G. R., Cook, W. H., 1985, "Fracture characteristics of three metals subjected to various strains, strain rates, temperatures and pressures," *Engineering Fracture Mechanics*, pp. 31-48.

16. Fish, J., Oskay, C., Fan, R., 2005, "Al 6061-T6 - Elastomer impact simulations" *Online Document* www.scorec.rpi.edu/cgi- bin/reports/Search3.pl?InputID=370

17. Jaspers, S.P.F.C, Dautzenberg, J.H., 2002, "Material behavior in conditions similar to metal cutting: flow stress in the primary shear zone" *Journal of Materials Processing Technology*, pp. 322-330.

18. Retrieved material properties April 15, 2009 from http://www.matweb.com

19. Elmer, J. W., Palmer, T. A., Babu, S. S., Zhang, W., Debroy, T., 2004, "Direct observations of Austenite, Bainite and Martensite formation during arc welding of 1045 Steel using time-resolved X-ray diffraction" *Welding Journal*, pp. 244s-253s

Chapter 6

PLUNGE EXPERIMENT WITH DONOR MATERIALS

A proof of concept experiment was carried out to demonstrate the feasibility of the donor material concept [1, 2, 3]. The materials selected for this experiment were copper as donor and AA 2024-T3 as the base material. These materials were selected based on the limitations of the modified milling machine which restricted plunges into any grade of steel. The significant difference in the hardness of copper and AA 2024-T3 coupled with the good thermal conductivity of copper made this combination a simple yet effective preliminary experiment for testing the concept.

6.1 *Experiment Set-up*

The purpose of this experiment was to compare the temperatures and axial load during a plunge into a combination of a copper and AA 2024 and a plunge into only AA 2024 of equal thickness. The equipment used for the experiment is described in Chapter 4. The axial force and temperature during the plunge were measured using a load cell and thermocouples. The experimental setup is shown in Fig. 6-1 and the thermocouple placement is shown in Fig. 6-2 [1, 2, 3]. The experiments were performed on a 38.1 mm x 38.1 mm x 9.525 mm thick AA 2024 used as the base material and a 38.1 mm x 38.1 mm x 3.175 mm thick copper piece placed on top of it. The copper was used as the donor material. Since the tool allowed a plunge depth of 6.35 mm, this meant that 50% of the plunge was into the donor material. A 2 mm x 2 mm groove was machined on to the trailing and leading side of the AA 2024 piece to accommodate the thermocouples. These grooves were positioned so as to measure temperature at the interface of copper and

aluminum. The thermocouples were placed along the grooves, 2 mm away from the pin. The temperature was measured using glass insulated Omega 20 gauge K-type thermocouples. The thermocouples and the load cell were connected to the DAQ using a 50 channel connector board. The temperature data from the thermocouples was converted to a milliVolt (mV) output based on the calibration charts from Omega, to make them compatible with the mV output of the load cell.

The primary challenge during the experiment was to hold the copper and aluminum plates together. Several different approaches were adopted to achieve this objective. Initially, the two plates were arranged with the aluminum at the top and the copper placed underneath with a lateral clamping force applied by a vise. It was expected that the vise would hold the plates together transversely and the vertical force from the plunge would suffice to keep the plates together during the experiment. However, upon plunging, the copper piece was warped, thus producing erroneous data. In order to remedy this, the plates were glued together at the four corners of the interface as shown in Fig.6-3. Extreme care was taken not to apply any adhesive in the plunge region as this could alter the dynamics of the process. Subsequently, the entire assembly was allowed to cure for at least 24 hours. At the end of this period, the assembly appeared strong enough during a manual peel test. Upon plunging, the two plates stayed together for a while but subsequently the copper piece started to warp. There are a few possible explanations to this behavior. Since the first part of the plunge was through the donor (copper), it started expanding very rapidly resulting in a high shear force between the two plates causing the plates to slide with respect to each other. The glue weakened at high temperature and

could not prevent this movement of the copper piece. As the copper started to expand and warp, the gap between the plates started to fill with flowing copper, exacerbating the warping. Finally the plates were fastened together with 4-40 3/8" size machine screws at the four corners. The arrangement of the two plates is shown in Fig. 6-4. The screws were sufficient to provide a good clamping force between the two plates and resist warping of the copper. This also provided a good thermal contact between the donor and the base material. This of course is important to ensure that the heat generated by a plunge into the donor is transferred rapidly into the base material.

While designing this set of experiments for the donor material, it became evident that an effective method of securing the donor material to the base material was crucial to the success of this technique. The securing method would ideally be simple to install, cutting down on the pre-processing time and yet provide a strong contact between the two materials for good heat transfer. As the process involves heat conduction between the donor and the workpiece material, a good thermal contact between the two is critical to the process' success. A possible method to improve this thermal contact would be the application of thermally conductive grease between the contact surfaces of the donor and the workpiece. This is a simple and cost-effective approach to ensure efficient heat transfer between the donor and the workpiece.

6.2 *Results and Discussion*

In the donor material experiment, the tool was penetrated first into the donor material and subsequently into the workpiece. The plunge was continued until the tool

shoulder made contact with the donor material. The tool was then allowed to spin without moving forward. As mentioned earlier during the plunge experiments, the machine was only capable of manual plunge, which resulted in different plunge times during each run. Fig. 6-5 shows the specimen at the end of the plunge. Experiments were also performed into a workpiece of AA 2024 without using a donor material to compare the results with the donor material experiment. The plunge into copper and AA 2024 combination took around 11 seconds to complete while the plunge into a AA2024 workpiece was achieved in approximately 20 seconds. The approximate average plunge speed in a donor and workpiece combination was estimated to be around 0.58 mm/sec and into a AA 2024workpiece it was estimated at 0.3175 mm/sec. It is interesting to note here that since the plunge was made manually, it was observed that it was significantly more difficult to plunge into a regular AA 2024 workpiece than into a workpiece with a donor material. The tool was then allowed to dwell for a little over 70 sec prior to retraction. A significantly long dwell period was added at the end of the plunge in order to reach a steady state condition for the axial load on the tool and temperature in the tool's vicinity. All the plunges were made with the milling machine head set at a 3^{o} angle. The LabView program was started approximately 8 sec before the plunge was initiated. This was done to allow the data acquisition system to stabilize before measurements were made.

Fig.6-6 compares the variation of axial load (kN) with time (sec) in the case of donor (copper) and workpiece (AA 2024) combination and a AA 2024 workpiece alone. In the case of a donor and workpiece combination, the two separate peaks were observed. At approximately 3 secs after the plunge was initiated, a peak of 15.5 kN was observed.

This peak load corresponds to that of the copper acting as the donor. As the temperature in the copper increased, the peak load dropped until the tool made contact with the base material, AA 2024. As the tool penetrated the aluminum plate, the load began to rise to a peak of approximately 23.5 kN. This peak occurred at approximately 9 secs after the plunge was initiated and it took approximately 11 secs to complete the plunge. The occurrence of the peak load before the completion of the plunge is due to the slow plunge speed which allows the heat to conduct through the material and soften it down before the plunge is completed. This is consistent with the trend in the axial load observed in a plunge into AA2024 alone. Subsequent to this, the load began to drop until it reached a steady state value of approximately 9 kN around the 30 sec mark (22 sec after the plunge was initiated). In comparison, the peak load of the plunge into AA 2024 alone was 30 kN. During the dwell period the load dropped and stabilized at approximately 18 kN. From this experiment, the advantage of a donor assisted plunge is clearly evident. The peak load in case of the donor was reduced by 22 %. Additionally the stable load during the dwell was almost two times higher in case of a plunge into regular AA 2024.

Fig. 6-7 shows the variation of temperature (^{o}C) with time (sec) at the trailing and leading edges. For the first few seconds into the plunge, the temperature at both the trailing and leading sides were identical. However, as expected the temperatures on the trailing edge soon began to rise at a much faster rate than on the leading edge. The temperatures on both the leading and trailing sides rose steeply until slightly after the end of the plunge. Thereafter, the temperature gradient decreased significantly during the dwell period. Temperatures on both the leading and trailing edges stabilized around 22

sec after plunge initiation, which was approximately 11 secs into the dwell period. The temperature on the trailing side stabilized at approximately $360\ ^{0}C$ and on the leading side it was approximately $300\ ^{0}C$. The axial load also stabilized around the same time. This is possibly due to a thermomechanical stability attained by the process.

Fig. 6-8 compares the temperature on the trailing side during the plunge into AA 2024 only and combination of donor copper and AA 2024. In this case, the plunge into the combination of donor copper and AA 2024 was completed in approximately 11 secs, however, the plunge into AA 2024 took 20 secs to complete. It is evident that the temperature at the end of the plunge phase in case of AA 2024 was significantly higher than the temperature in the donor and workpiece combination. In the plunge into copper and AA 2024, the plunge into copper was completed approximately 5 secs after the initiation of plunge. The temperature at the interface, 5 secs after the initiation of plunge was approximately $140\ ^{0}C$ on the trailing side and $100\ ^{0}C$ on the leading side. Since these measurements were made 2 mm away from the pin, it is very likely that the temperature under the tool pin was even higher. Therefore, it is evident that the plunge area of AA 2024 was heated to a temperature higher than $140\ ^{0}C$ before the tool pin established contact with it. This localized pre-heating of the base material (AA 2024) was caused by conduction of the heat generated from the plunge into the donor material (copper). The base material became significantly softer due to the pre-heating thus resulting in lower axial loads during the plunge. From the discussion in Chapter 5, it is evident that lower axial loads would result in lower tool wear. Similar to the plunge experiments discussed in Chapter 4, a steady state condition for either axial load or

temperature was not attained during the plunge phase. However, with a sufficiently long dwell period it was observed that the axial load stabilized almost immediately after the plunge phase whereas the temperature continued to increase for a long period after the plunge was completed.

6.3 *Summary*

In the final phase of the research in this dissertation, a proof of concept experiment was carried out to demonstrate the feasibility of the donor material concept. The materials selected for this experiment were copper as donor and AA 2024-T3 as the base material with 50% of plunge through the donor. The axial force and temperatures were recorded during the plunge. The axial force during the plunge into a combination of donor and AA2024 was observed to be 21% less than a plunge into regular AA 2024. This demonstrates the effectiveness of the donor material concept in reducing the axial load and hence tool wear.

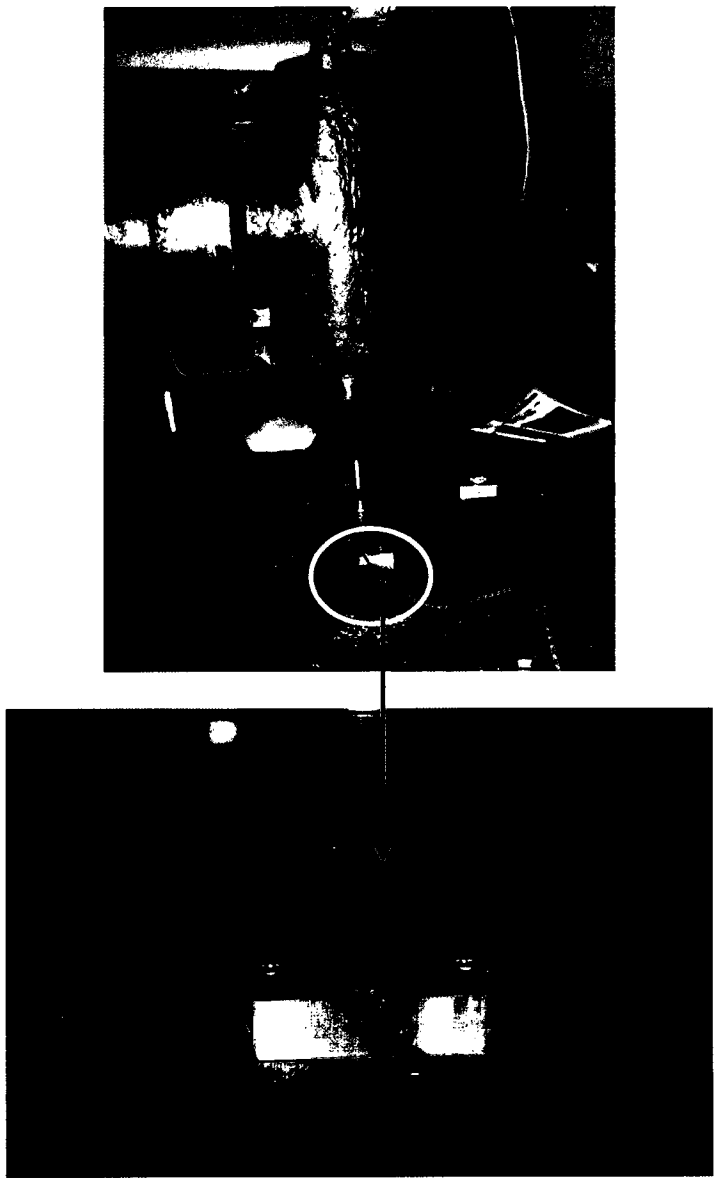

Fig. 6-1 Experimental setup for FSW plunge testing on AA2024 with a copper donor

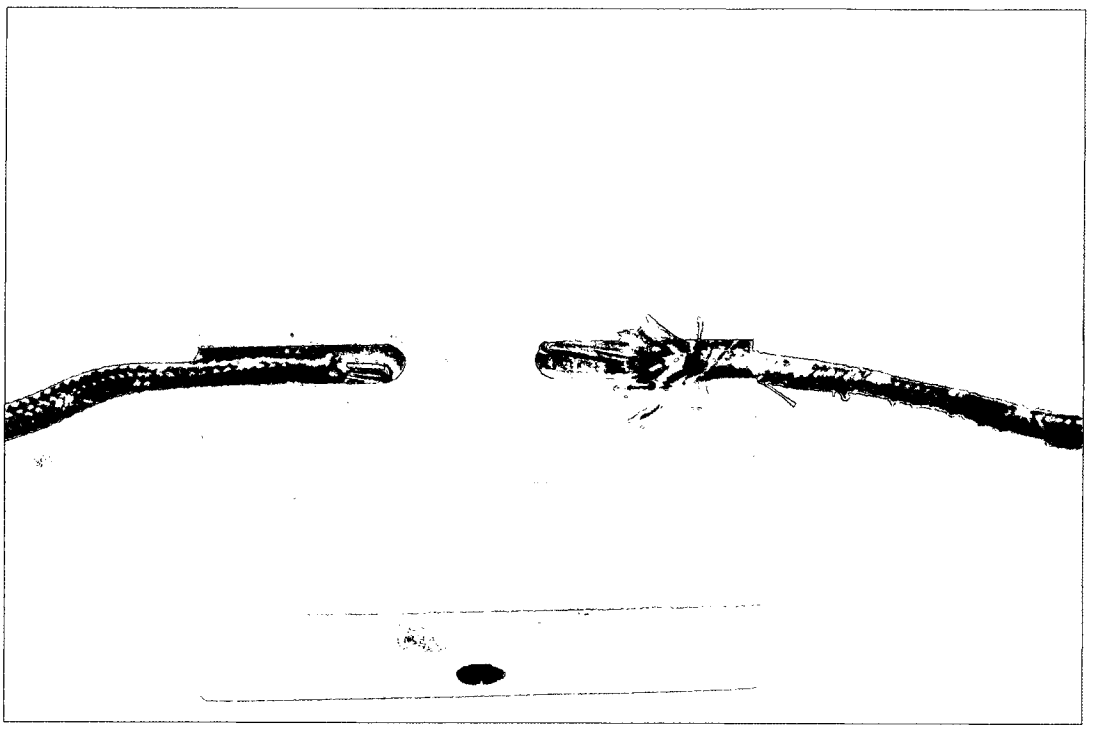

Fig. 6-2. Thermocouples positioned in machined slots in AA2024

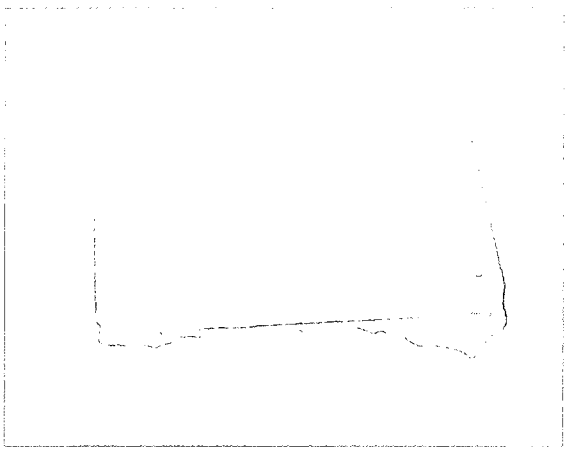

Fig. 6-3 a) Copper donor and AA 2024 glued together

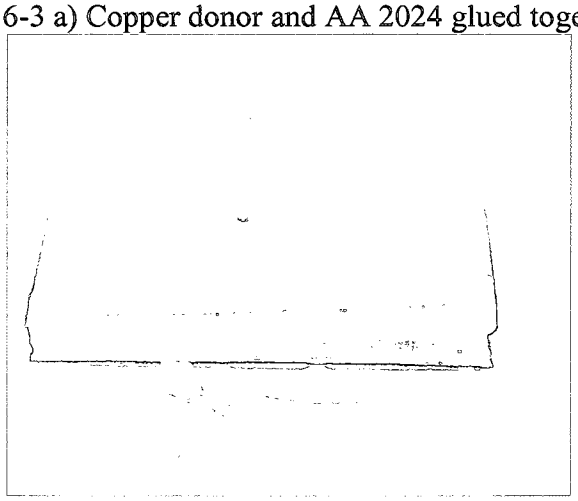

Fig. 6-3 b) Separation of donor and workpiece after plunge

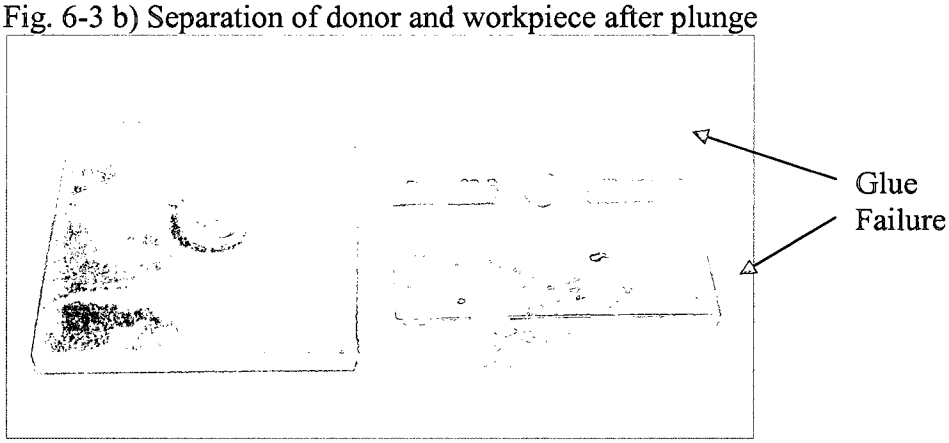

Fig. 6-3 c) Donor and workpiece separated after glue failure

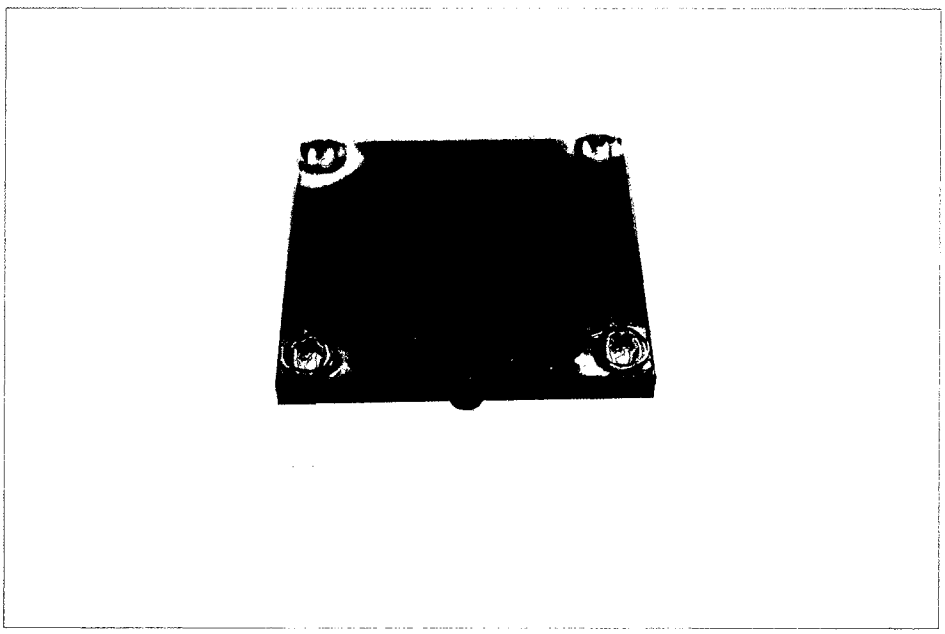

Fig. 6-4 Copper donor and AA 2024 fastened together with screws

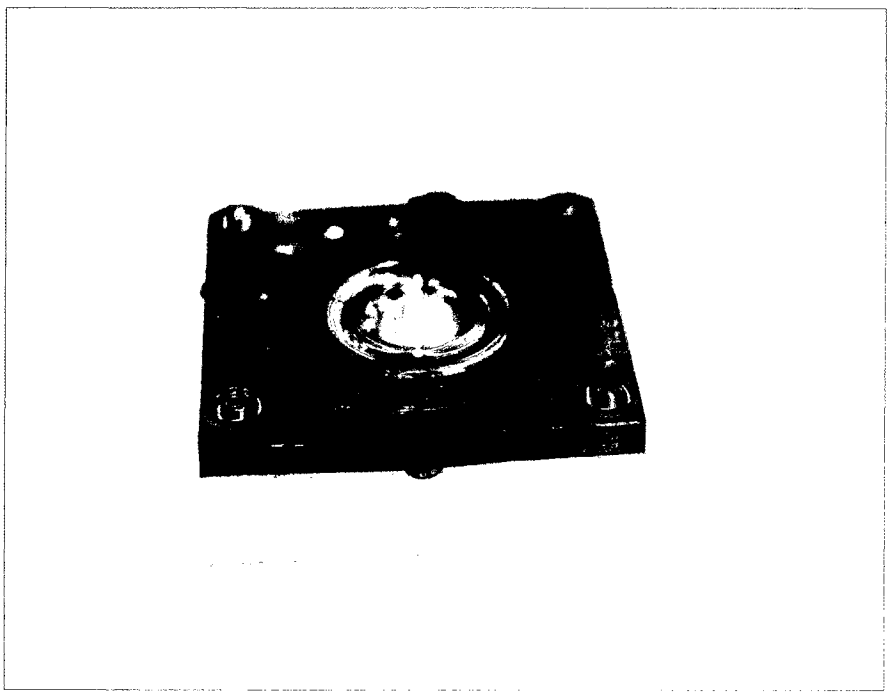

Fig. 6-5 Specimen at the end of a plunge

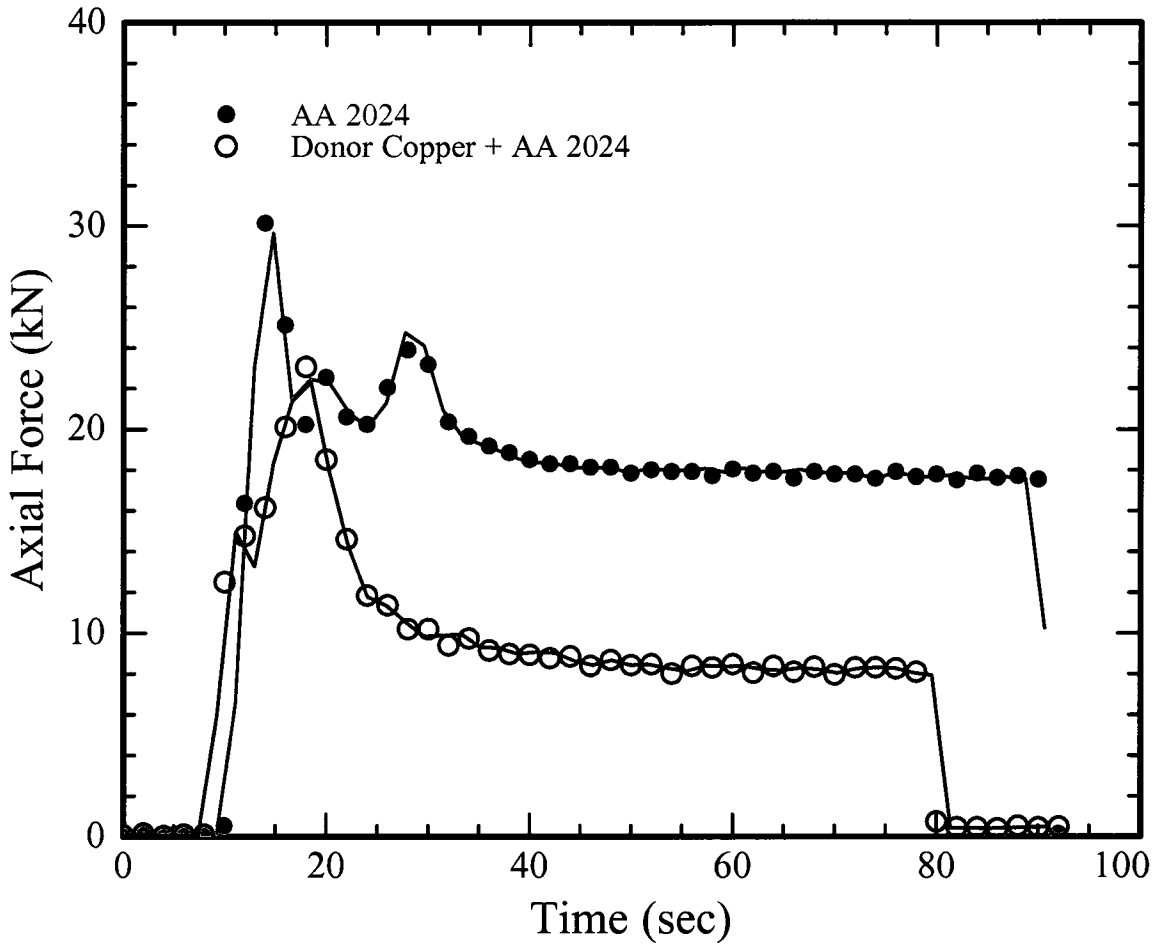

Fig. 6-6 Variation of axial load in case of plunge into AA 2024 with and without a copper donor

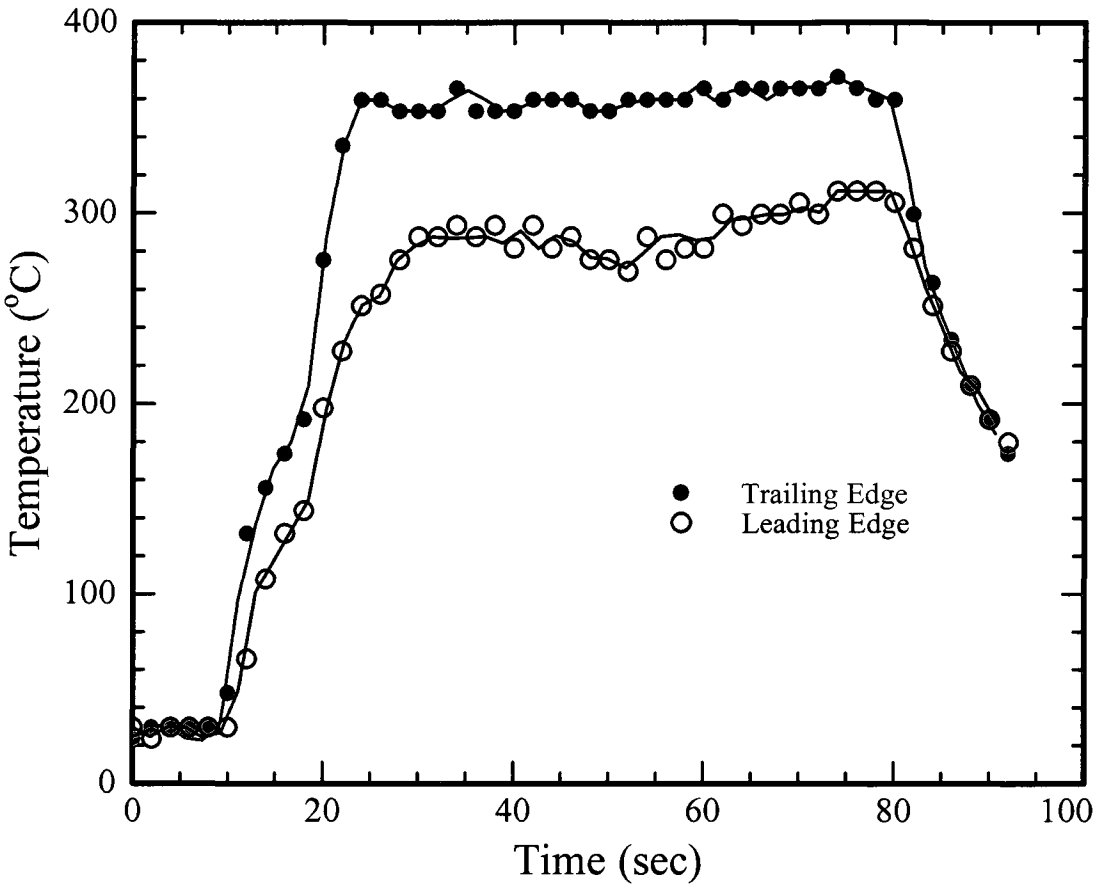

Fig. 6-7 Temperature data from donor experiment

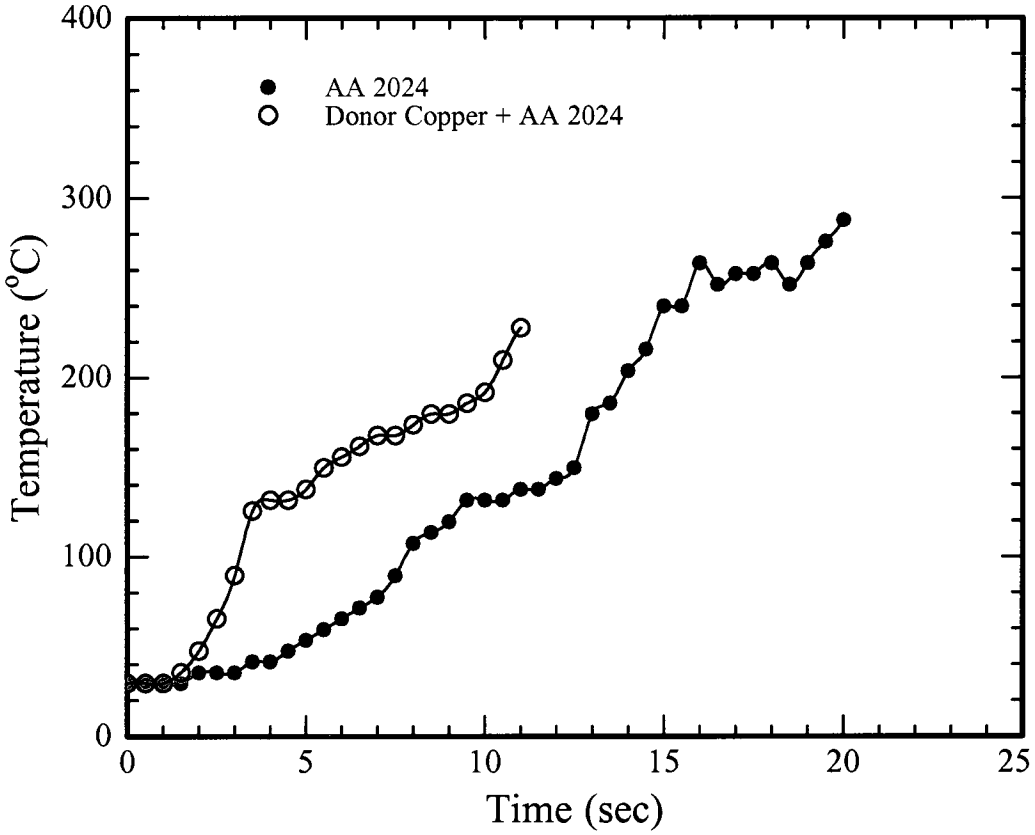

Fig. 6-8 Temperature comparison during experimental plunge into AA 2024 only and combination of Donor Copper + AA 2024

References:

1. Donor material technology for friction stir welding, U.S. Provisional Patent Application No. 61/070,642.

2. Mandal, S., Rice, J. Elmustafa, A.A., "Donor material concept for reducing tool wear in FSW – a numerical and experimental investigation" *In preparation*

3. Rice, J., 2009, "A three dimensional numerical investigation of a donor material in friction stir welding" *M.S. Thesis*, Old Dominion University.

Chapter 7

CONCLUSION

In the first part of this research, the plunge phase of FSW was investigated numerically and experimentally. The second part presented a novel concept for reducing tool wear called the 'donor material concept.' This concept was numerically simulated and a proof of concept experiment was demonstrated. The current chapter briefly reviews the highlights from this research.

- A numerical investigation was performed on the plunge stage of friction stir welding. The plunge phase is crucial as it generates the initial thermomechanical conditions in the material. ABAQUS was used to construct a numerical model with the strain-rate and temperature dependent Johnson-Cook law as the material constitutive law. The simulations were compared with experimental results obtained from literature. The calculated temperature from the model correlated well with the experimental data from the literature. To improve the correlation between the experimental data and numerical simulation of the axial force, the model could be remeshed with a higher mesh density, which would lead to a higher computational time. This research constitutes a significant step in the direction of the study of thermomechanical conditions in the plunge area and forms the foundation for the development of the donor material concept to reduce tool wear.

- In the subsequent part of the research on the plunge phase of FSW, experiments were conducted by plunging into coupons of aluminum alloy 2024-T3 and the temperatures and axial load were measured. The results from these experiments were different from the first FEA simulation as well as experiments conducted by Gerlich et al due to the fact that these experiments were conducted using a manually controlled milling machine resulting in significantly slower plunge rates. Also, a second FEA model was constructed to compare with the present set of experiments. A good correlation was observed for the first 5 sec of the plunge after which the simulation suffered convergence problems.

- The second part of this dissertation proposes a novel concept for providing localized pre-heating of the workpiece material in the plunge region in order to mitigate tool wear. The tool penetrates through a softer donor material, generating heat due to friction and plastic work in the donor material. The generated heat is transferred into the harder workpiece material beneath the donor by conduction. This pre-heats the workpiece at the plunge area resulting in material softening. A softer workpiece material would result in lower flow stresses in the material, thus reducing wear. A numerical investigation was performed on the effect of placing a softer donor material on top of a 1045 steel workpiece. Three different donor materials, AA 2024, AA 6061 and copper were discussed. The donor materials were positioned so that they formed 50% and 75% of the plunge depth. It was observed that the axial load during the plunge decreased by approximately 80%.

Additionally the contact stresses at the tool workpiece interface also decreased by approximately 75% when a donor material was used in the plunge area.

- In the final phase of research, a proof of concept experiment was carried out to demonstrate the feasibility of the donor material approach. The materials selected for this experiment were copper as donor and AA 2024-T3 as the base material. The axial force and temperatures were recorded during the plunge. The axial force during the plunge into a combination of donor and AA2024 was observed to be as much as 21% less than a plunge into AA2024.

Chapter 8

FUTURE RESEARCH

Although FSW has largely been confined to welding softer materials, the scope of using this technology to weld high hardness materials such as steel is unequivocal. Several researchers have already demonstrated the feasibility of welding steel but the challenge remains in producing long welds of consistent quality particularly for the shipbuilding industry. Tool wear and the frequent replacement of tools make the cost of FSW prohibitive in the case of steels. This dissertation proposes an economical concept to mitigate tool wear at the plunge region where most of the wear occurs. There are also other approaches to mitigate tool wear at various stages in the process. The use of high-strength tools is a popular approach. This seems to be a logical approach since the FSW process depends on a significant hardness difference between the tool and the workpiece. However, high hardness materials are also typically associated with a low toughness. So the susceptibility of these tools to fracturing complicates the process. The use of a thermo-mechanical hot channel to pre-heat the entire joint line of the weld is another feasible approach. However, a cost effective solution to countering tool wear in high hardness materials is a combination of all the above approaches. The use of the donor material concept coupled with a thermo-mechanical hot channel along the weld line would reduce the hardness of the material both at the plunge region and along the weld line. This would reduce the extremely high hardness requirement on the tool. A lower hardness but higher toughness carbide based tool as opposed to the typical PCBN would suffice in producing high quality welds in steels.

Although the concept of donor material to reduce tool wear has been demonstrated in this dissertation, the process needs to be optimized in order for it to be economically viable for industrial production purposes. This dissertation uses a largely theoretical approach in the placement of the donor material but research needs to be done to develop a process to efficiently position the donor material at the start of the weld. Also, the thickness of the donor material required for a particular application is a research topic in its own merit. The thickness is likely to depend on the properties of the workpiece to be welded and an optimal donor to workpiece thickness ratio needs to be developed.

Along with the development of a feasible process to stir weld steels, it is also crucial to understand the mechanism of tool wear in FSW. From the discussions in Chapter 2 and Chapter 5, it is evident that a significant amount of research has been done in understanding tool wear mechanisms in common machining processes. Numerical models to better understand these mechanisms in FSW are currently being developed [1].

References

1. Rice, J., 2009, "A three dimensional numerical investigation of a donor material in friction stir welding" *M.S. Thesis*, Old Dominion University.

CURRICULUM VITA
for
SAPTARSHI MANDAL

EDUCATION

Ph.D (Mechanical Engineering), Old Dominion University, Norfolk, Virginia, August 2009

MS (Mechanical Engineering), Old Dominion University, Norfolk, Virginia, August 2003

BE (Marine Engineering), Marine Engineering & Research Institute, Calcutta, India, August 2000

PROFESSIONAL CHRONOLOGY

Mechanical Engineer, Jefferson Lab, Newport News, Virginia
October 2007 – Present

Graduate Teaching Assistant, Old Dominion University, Norfolk, Virginia
August 2003 - May 2007

Graduate Research Assistant, Old Dominion University, Norfolk, Virginia
May 2001 - May 2004

PUBLICATIONS

S. Mandal, J. Rice , and A. A., Elmustafa, "Experimental and Numerical Investigation of the Plunge Stage in Friction Stir Welding", *Journal of Materials Processing Technology,* 2008 411- 419.

S. Mandal, and K. Williamson, "A thermomechanical hot channel approach for friction stir welding", *Journal of Materials Processing Technology*, 2006, pp.190-194.

S. Mandal, J. Rice , and A. A., Elmustafa, "Donor material concept for reducing tool wear in FSW – a numerical and experimental investigation", *In preparation*

S. Mandal, S. Kose, A. Frank, and A. A., Elmustafa, "A Numerical Study on Pile-up in Nanoindentation Creep", *International Journal of Surface Sciences*, 2008, pp. 41-51.

S. Mandal, J. Rice, and A. A. Elmustafa, "A Numerical Study of The Plunge Stage in FSW Using ABAQUS", *Proceedings of Friction Stir Welding and Processing IV*, TMS, 2007.

S. Mandal, K. Williamson and G. Hou, "Over-stirring Hole Defects during Thermomechanical Stir Processing", *Proceedings of Friction Stir Welding and Processing II*, TMS, 2003.

AWARDS

University Graduate Fellowship, Old Dominion University, August 2005.